ORIGINAL RESEARCH

Neuroprotective Effect of Melatonin in a Neonatal Hypoxia–Ischemia Rat Model Is Regulated by the AMPK/mTOR Pathway

Efe Nacarkucuk [iD]*; Maria E. Bernis, PhD*; Anna-Sophie Bremer; Kora Grzelak; Margit Zweyer [iD]; Elke Maes; Hannah Burkard; Hemmen Sabir, MD

BACKGROUND: Melatonin has been shown to be neuroprotective in different animal models of neonatal hypoxic–ischemic brain injury. However, its exact molecular mechanism of action remains unknown. Our aim was to prove melatonin's short- and long-term neuroprotection and investigate its role on the AMPK (AMP-activated protein kinase)/mTOR (mammalian target of rapamycin) pathway following neonatal hypoxic–ischemic brain injury.

METHODS AND RESULTS: Seven-day-old Wistar rat pups were exposed to hypoxia–ischemia, followed by melatonin or vehicle treatment. Detailed analysis of the AMPK/mTOR/autophagy pathway, short- and long-term neuroprotection, myelination, and oligodendrogenesis was performed at different time points. At 7 days after hypoxia–ischemia, melatonin-treated animals showed a significant decrease in tissue loss, increased oligodendrogenesis, and myelination. Long-term neurobehavioral results showed significant motor improvement following melatonin treatment. Molecular pathway analysis showed a decrease in the AMPK expression, with a significant increase at mTOR's downstream substrates, and a significant decrease at the autophagy marker levels in the melatonin group compared with the vehicle group.

CONCLUSIONS: Melatonin treatment reduced brain area loss and promoted oligodendrogenesis with a clear improvement of motor function. We found that melatonin associated neuroprotection is regulated via the AMPK/mTOR/autophagy pathway. Considering the beneficial effects of melatonin and the results of our study, melatonin seems to be an optimal candidate for the treatment of newborns with hypoxic–ischemic brain injury in high- as well as in low- and middle-income countries.

Key Words: AMPK/mTOR/autophagy ■ melatonin ■ neonatal hypoxia–ischemia ■ neuroprotection ■ rat

Neonatal hypoxic–ischemic encephalopathy (HIE) has an incidence of approximately 3 to 5 neonates per 1000 live births in high-income countries, and it is 10 to 20 times higher in low- and middle-income countries (LMICs).[1] Depending on the severity of brain injury, newborns can develop lifelong morbidities such as epilepsy, cerebral palsy, and behavioral disorders.[2,3]

At the moment, the current standard therapeutic option used in moderate–severe neonatal HIE cases is therapeutic hypothermia (TH).[4,5] However, its effectiveness is limited depending on the severity of the brain insult or the presence of several conditions such as infectious/inflammatory situations.[6] Cooling should be initiated within the first 6 hours of life[7]; however, in LMICs, initiation of TH can be delayed for many reasons.[8] Owing to these shortcomings, in addition to its beneficial effects, the development of promising alternative approaches could save more newborn lives, especially in LMICs.

RESEARCH PERSPECTIVE

What Is New?

- To our knowledge, this is one of the first studies to evaluate the relationship between melatonin treatment and the AMPK (AMP-activated protein kinase)/mTOR (mammalian target of rapamycin) pathway, in particular the broad spectrum downstream of the molecular pathway, in a rat model of neonatal hypoxic–ischemic brain injury.
- Our study fully investigated the possible molecular mechanisms involved in the neuroprotective effects of melatonin, although the neuroprotective effect of melatonin has been previously demonstrated.
- Our findings demonstrate that melatonin treatment has clear neuroprotective effects, particularly in the reduction of brain area loss, motor function improvement, oligodendrogenesis, and remyelination, and triggers regulation of the AMPK/mTOR/autophagy pathway after neonatal hypoxia–ischemia insult.

What Question Should Be Addressed Next?

- We believe that our current study, owing to its contribution to previous studies, elucidates one of the potential mechanisms underlying the observed neuroprotective effects and may help to understand how melatonin's neuroprotective effects are regulated at the molecular level, leading to improvements in current preclinical/clinical treatments for neonatal hypoxic–ischemic encephalopathy, as well as in the development of new therapeutic options, guiding further preclinical and clinical studies in this field and helping to save millions of babies worldwide.

Nonstandard Abbreviations and Acronyms

4-EBP1	eukaryotic translation initiation factor 4E (eIF4E)-binding protein 1
AMPK	AMP-activated protein kinase
CC1	adenomatous polyposis coli APC
GFAP	glial fibrillary acidic protein
HI	hypoxia–ischemia
HIE	hypoxic–ischemic encephalopathy
HIF1α	hypoxia-inducible factor 1α
Iba1	ionized calcium binding adaptor molecule 1
LMIC	low- and middle-income country
MAP1LC3/LC3	microtubule-associated protein 1 light chain 3
MBP	myelin basic protein
mTOR	mammalian target of rapamycin
mTORC1	mammalian target of rapamycin complex 1
NF-κβ	nuclear factor-κβ
NLRX1	nucleotide-binding oligomerization domain and leucine-rich repeat-containing protein X1
NOR	novel object recognition
Olig2	oligodendrocyte-2
p4EBP-1	phosphorylated eukaryotic translation initiation factor 4E (eIF4E)-binding protein 1
p62	sequestosome 1
p-AMPK	phosphorylated AMP-activated protein kinase
p-mTOR	phosphorylated mammalian target of rapamycin
p-S6	phosphorylated S6
p-ULK-1 (S555)	phosphorylated ULK-1 serine 555
p-ULK-1 (S757)	phosphorylated ULK-1 serine 757
S6K	S6 kinase
SQSTM1	sequestosome 1
TH	therapeutic hypothermia
ULK-1	uncoordinated-51-like kinase 1

AMPK (AMP-activated protein kinase) and mTORC1 (mammalian target of rapamycin complex 1) play major roles in regulating cellular energy metabolism.[9] AMPK and mTOR can sense the energy status of cells, and their activation depends on their phosphorylation.[9] Both molecular pathways regulate many cellular mechanisms such as cell survival, autophagy, and the cell cycle.[9] During hypoxic-ischemic conditions, activated AMPK inhibits mTORC1,[9–12] which then regulates downstream substrates such as eIF4E (eukaryotic translation initiation factor 4E)-4EBP-1 (binding protein 1) and S6K (S6 kinase), both of which are involved in cap-dependent translation.[13,14] In addition, regulation of the AMPK/mTOR pathway also plays a key role in the regulation of autophagosome proteins like ULK-1 (uncoordinated-51-like kinase 1), MAP1LC3 or LC3 (microtubule-associated protein 1 light chain 3), and SQSTM1 (sequestosome 1)/p62.[15] The phosphorylation of ULK-1 in the serine 555 subunit by AMPK drives cellular autophagy.[9,15] On the

other hand, phosphorylation of ULK-1 at serine 757 by mTORC1 inhibits ULK-1 and blocks autophagy.[15,16] HIF1α (hypoxia-inducible factor 1α) and NF-κβ (nuclear factor-κβ) are 2 of the many transcription factors regulated by mTOR and hypoxic conditions.[17–19]

Melatonin (N-acetyl-5-methoxytryptamine), an indolamine hormone, is mainly secreted by the pineal gland and can be synthesized in several ways.[20] Its secretion follows a circadian rhythm, with nocturnal secretion reaching its peak level.[21] Its beneficial effects include the ability to cross the blood–brain barrier easily; strong safety profile; and antioxidative, antiapoptotic, and anti-inflammatory features, making it a good candidate for neonatal HIE treatment in high- and low-income countries.[22–24]

In the present study, we aimed to explore the neuroprotective mechanism of melatonin as a potential compound in the treatment of neonatal HIE and characterized the regulatory mechanism of AMPK/mTOR as a potential mode of action regulated after melatonin treatment.

METHODS

All data can be accessible via the corresponding author.

Animal Handling

All experimental protocols were approved by the Animal Protection Committee of the State Environment of North Rhine, Westphalia, Germany under animal licenses AZ 81–02.04.2018.A166 and AZ 81–02.04.2022.A174.

The article is written in accordance with the Animal Research: Reporting of in Vivo Experiments guidelines.

All experiments were conducted using 7-day-old (P7) Wistar rat pups of both sexes (Figure 1). All animals were housed in the central animal laboratory facility of the Deutsches Zentrum für Neurodegenerative Erkrankungen, Bonn, Germany, at an ambient temperature of 21 °C, with a 12-:12-hour dark/light cycle, and accessibility to adequate food and water at any time (ad libitum). All animals were randomized across litter, weight, and sex for all treatments before the initiation of the experiments. All experimental and analysis processes were executed by observers blinded to the different treatments.[25,26]

Animal Experiment Procedure

A total of 137 animals from different therapeutic groups were used in this study and were euthanized at different time points (see Table 1).

Temperature monitoring was performed using a rectal probe (IT-21; Physitemp Instruments, Clifton, NJ) connected to a servo-controlled cooling machine and a cooling mat (CritiCool; MTRE, Yavne, Israel) with sentinel rat pups that were not included in the treatment groups.[25,26] The sentinel pups maintained the nesting temperature of P7 rat pups[27] or treatment temperatures during all the experiments (see below). The standardized hypoxia–ischemia (HI) Vannucci rat model was used for this study, as previously published.[25,26] Briefly, animals were injected with buprenorphine (0.1 mg/kg) 30 minutes before surgery. Left common carotid artery ligation was performed under isoflurane anesthesia using
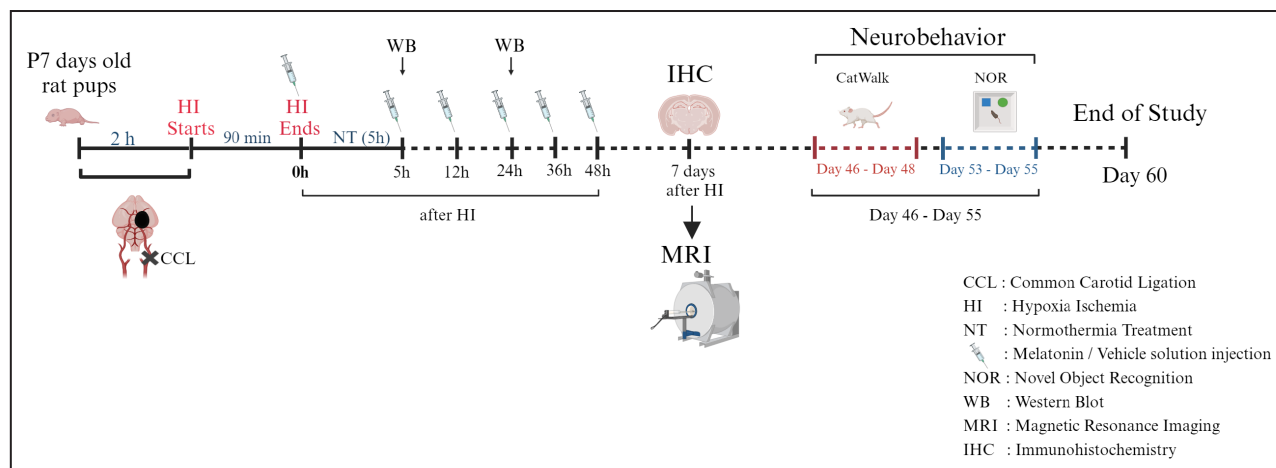
Figure 1. **Schematic design of the present study.**

P7 Wistar rat pups underwent left common carotid artery ligation under isoflurane anesthesia. After surgery, the pups were placed in a hypoxia chamber with 8% O$_2$ for 90 minutes. At the end of hypoxia, the pups were treated with normothermia for 5 hours. Except for the sham group, the pups were injected with melatonin or vehicle solution at a dose of 25 mg/kg at 0, 5, 12, 24, 36, and 48 hours after HI. At 5 and 24 hours after HI, the animals were euthanized for Western blot analysis. Seven days after HI (P14), IHC and MRI were performed. The pups that were scanned using MRI were maintained for neurobehavioral tests between days 46 and 55. The study was completed on day 60. CCL indicates common carotid ligation; HI indicates hypoxia–ischemia; IHC, immunohistochemistry; MRI, magnetic resonance imaging; NOR, novel object recognition; NT, normothermia treatment; P7, 7 days old; P14, 14 days old; and WB, Western blot.

Table 1. Number of Animals Used Per Condition

Purpose	Treatment	Time points (after HI)	N	Mortality, N	Exclude, N
Western blot	HI/vehicle	5 h	9	…	…
	HI/melatonin	5 h	15	2*	1†
	HI/vehicle	24 h	9	…	…
	HI/melatonin	24 h	15	2*	1†
Immunohistochemistry	HI/vehicle	7 d	15	2 (1‡ and 1*)	8§
	HI/melatonin	7 d	15	…	9§
Pharmacodynamic	HI/melatonin	0 h	4	…	…
	HI/melatonin	1 h	5	…	…
	HI/melatonin	2 h	5	…	…
	HI/melatonin	4 h	5	…	…
	HI/melatonin	8 h	4	…	…
	HI/melatonin	24 h	6	…	…
Neurobehavior	HI/vehicle	Between 41 and 48 d	16	4 (3* and 1‡)	…
	HI/melatonin		14	1*	…

H indicates hypoxia–ischemia.

*Died during or after hypoxia.

†Excluded due to insufficient amount of protein for biochemistry analyses.

‡Died during ligation.

§The brain regions analyzed were severely damaged.

a dissection microscope. After common carotid artery ligation, animals were subjected to hypoxia (8% O_2) for 90 minutes at a rectal temperature of 36 °C in the hypoxia chamber.[25,26] After HI, all animals were exposed to normothermia treatment at a rectal temperature of 37.0 °C for 5 hours, as previously defined.[5,25,26] Following the treatment processes, the pups were returned to their dams and euthanized at different time points (see Table 1) using a single intraperitoneal dose of chloralhydrate injection (450 mg/kg). The sham group received only isoflurane anesthesia for 5 minutes.

Melatonin and Vehicle Solution Injections

A single IP injection of melatonin at a concentration of 25 mg/kg was administered at 0, 5, 12, 24, 36, and 48 hours after HI. An ethanol-free excipient solution (CHIESI Pharmaceuticals, Parma, Italy) was used as the vehicle control group under the same dosage regime as melatonin and was dissolved in an ethanol-free solution.[28] The timing and dosing was based on our primary study showing neuroprotection of melatonin with the dosing regimen.[29]

Biochemistry Analysis

To perform Western blot, pups were euthanized at 5 hours (after 2 doses of melatonin or vehicle injections [25 mg/kg each]) and 24 hours (after 4 doses of melatonin or vehicle injections [25 mg/kg each]) after HI.

The cortical and hippocampal areas were lysed in radioimmunoprecipitation buffer in addition to phosphatase and protease inhibitors. The bicinchoninic acid assay (PierceTM; Thermo Fisher Scientific) was used to measure the total protein concentration according to the manufacturer's instructions. With a few modifications, immunoblotting was performed as defined in advance.[26] Fifty micrograms of total protein were loaded onto a Bis-Tris 10% gel, and a 2-morpholinoethanesulfonic acid buffer system (Thermo Fisher Scientific) was used to perform SDS-polyacrylamide gel electrophoresis. Then, protein transfer was performed using a polyvinylidene difluoride membrane overnight at 4 °C and 30V using a transfer buffer containing 10% methanol. The membranes were blocked either with 5% (w/v) milk (for nonphosphorylated proteins) or 5% (w/v) bovine serum albumin (for phosphorylated proteins) in TBS with 0.05% Tween-20 for 1 hour at room temperature, following incubation with primary antibody overnight at 4 °C in 1% (v/v) blocking buffer (see Table 2). Secondary goat anti-mouse (IRDye 680) and goat anti-rabbit (IRDye 800) antibodies (see Table 2) were used to develop membranes (Invitrogen). To image membranes, the Odyssey infrared imaging system (LI-COR Biosciences) was preferred. ImageJ software was used to determine the optical density, which was further normalized to β-actin as a loading control. The ratio was calculated based on the amount of phosphorylated protein compared with the total protein content.

Some of the membranes were reincubated with primary and secondary antibodies to analyze different proteins, and mild-stripping was performed using mild-stripping buffer, which contains glycine 200 mmol/L (Roth), SDS (0.1% v/v; Roth), and Tween 20 (0.1% v/v, Sigma-Aldrich), followed by washing, blocking, and incubating steps, as described above.

Some of the proteins analyzed in this study contained 2 bands (ie, 4-EBP1 and LC3), which are

Table 2.   List of Antibodies Used for Biochemistry (Western Blot) and Immunohistochemistry

Technique	Name of the antibodies	Catalog no.	Company	Host	Dilution	Clone	Molecular weight, KDa
Western blot	AMPK	2532	Cell Signaling Technology	Rabbit	1:500	…	62
	Phospho AMPK Thr172	2535	Cell Signaling Technology	Rabbit	1:500	40H9	62
	mTOR	2983	Cell Signaling Technology	Rabbit	1:500	7C10	289
	Phospho mTOR Ser2448	2974	Cell Signaling Technology	Rabbit	1:500	…	289
	4EBP-1	9644	Cell Signaling Technology	Rabbit	1:500	53H11	15–20
	Phospho 4EBP-1 Thr37/46	2855	Cell Signaling Technology	Rabbit	1:500	236B4	15–20
	S6 ribosomal	2217	Cell Signaling Technology	Rabbit	1:500	5G10	32
	Phospho S6 ribosomal Ser240/244	5364	Cell Signaling Technology	Rabbit	1:500	D68F8	32
	NF-κβ	8242	Cell Signaling Technology	Rabbit	1:1000	D14E12	65
	HIF1α	GTX127309	GeneTex	Rabbit	1:500	…	93
	ULK-1	6439	Cell Signaling Technology	Rabbit	1:500	D9D7	113
	Phospho ULK-1 S555	58695	Cell Signaling Technology	Rabbit	1:500	D1H4	113
	Phospho ULK-1 S757	14202	Cell Signaling Technology	Rabbit	1:500	D706U	113
	LC3	14600-1-AP	Proteintech	Rabbit	1:1000	…	14–18
	p62	ab109012	Abcam	Rabbit	1:1000	EPR4844	62
	β-Actin	A1978	Sigma-Aldrich	Mouse	1:3000	…	45
	Goat anti-rabbit IgG secondary antibody, DyLight 800	SA535571	Thermo Fisher	Rabbit	1:5000	…	…
	Goat anti-mouse IgG secondary antibody, DyLight 680	35518	Thermo Fisher	Mouse	1:3000	…	…
Immunohistochemistry	Iba1	019–19741	FUJIFILM Wako	Rabbit	1:400	…	…
	GFAP	80788	Cell Signaling Technology	Rabbit	1:100	E4L7M	…
	MBP	ab218011	Abcam	Rabbit	1:500	EPR21188	…
	Anti-APC antibody/CC1	ABIN3183309	Antibodies-Online	Rabbit	1:100	…	…
	Olig2	AB9610	Merk	Rabbit	1:200	…	…
	Goat anti-mouse IgG, IgM secondary antibody, Alexa Fluor 488	A11008	Thermo Fisher	Mouse	1:400	…	…

4EBP-1 indicates eukaryotic translation initiation factor 4E (eIF4E)-binding protein 1; AMPK, AMP-activated protein kinase; APC, adenomatous polyposis coli; CC1, adenomatous polyposis coli APC; GFAP, glial fibrillary acidic protein; HIF1α, hypoxia-inducible factor 1α; Iba1, ionized calcium binding adaptor molecule 1; IgG, immunoglobulin G; IgM, immunoglobulin M; LC3, microtubule-associated protein 1 light chain 3; MBP, myelin basic protein; mTOR, mammalian target of rapamycin; NF-κβ, nuclear factor-κβ; Olig2, oligodendrocyte-2; S555, serine 555; S757, serine 757; Ser, serine, p62, sequestosome 1; Thr, threonine; and ULK-1, uncoordinated-51-like kinase 1.

expressing 2 different subforms (ie, LC3-I and LC-II), and both of the bands were included in the analyses (see Table 2).[9,15]

Histology and Immunohistochemistry

At the final time points (7 and 60 days after HI), animals were perfused by transcardiac fixation with 10% neutral-buffered formalin, and all brains were preserved in 10% neutral-buffered formalin until further processing. Coronal blocks were cut into 3-mm sections and following the sectioning process embedded in paraffin. Slices were cut at a 10-μm thickness from 2 adjacent blocks representing the cortex, hippocampus, thalamus, and basal ganglia (distance to Bregma, −3.8 mm). Hematoxylin and eosin staining was performed, and

the sections were scanned using an Epson Perfection V750 Pro. Analysis of the hemispheric area was performed using ImageJ software. Following comparison of the ipsilateral and contralateral sides, the area loss of the ligated side was estimated using the formula (1−(left area/right area)×100), as previously defined.[25]

Immunohistochemistry was executed in brain samples 7 days after HI, as previously defined[25,26] (see Table 1). For immunohistochemistry analyses, some brains were excluded because some areas in the ipsilateral brain were too severely injured, and technical preparation of the brain sites was not feasible (data not shown). After deparaffinization of coronal sections (approximately at −3.8±0.7 mm from Bregma), rehydration was performed. Antigen retrieval was performed using preheated PBS ×1 for 7 minutes, followed by permeabilization with 0.1% Triton X-100 for 30 minutes at room temperature. Slices were incubated with primary antibodies (see Table 2) in 0.7% carrageenan solution with 0.02% NaN$_3$ solution in PBS ×1 overnight at 4 °C after a blocking step with 20% normal goat serum in PBS ×1 (Invitrogen). The next day, incubation with the appropriate secondary antibody (see Table 2) was performed. Following this step, Fluoromount-G mounting medium with DAPI (Thermo Fisher Scientific) was used to counterstain sections. Images were taken using an AxioScan Z.1 microscope (Zeiss, Germany) with a ×20 objective or a confocal LSM800 microscope (Zeiss, Germany) with a ×20 objective and a zoom of ×2 to ×3. Furthermore, Z stacking was executed using an interval of 9 slices with a distance of 1 μm between each respective Z stack. ZEN Blue 3.1 (Zeiss) and ImageJ software were used for analysis, performing maximal projection to analyze and quantify the cells of interest. Different regions of the same coronal section (approximately at Bregma −3.8 mm) were drawn to create a fixed area. The cortex (especially the primary somatosensory cortex), corpus callosum, hippocampus (especially CA2-CA3 areas of the hippocampus), thalamus, and amygdala were the areas of interest because they represent the most affected areas after HI.[30] The following markers were used for the analysis: Iba-1 (ionized calcium binding adaptor molecule 1, microglia), CC1 (adenomatous polyposis coli APC, mature oligodendrocytes), and Olig2 (oligodendrocyte-2, immature oligodendrocytes), in which the number of cells per area was counted. GFAP (glial fibrillary acidic protein, astrocytes) and MBP (myelin basic protein, myelin sheet) were analyzed by measuring the maximal intensity per area. All analyses were corroborated by their respective nuclear staining with DAPI.

Magnetic Resonance Imaging

Magnetic resonance imaging (MRI) scans were performed 7 days after HI insult. An 11.7 T horizontal small-bore magnet (Biospec 117/16; Bruker, Billerica, MA) was chosen to perform MRI using a rat brain receive only proton (1H) coil (Bruker Biospin). A rapid acquisition relaxation enhancement T2-weighted sequence (echo time=25 milliseconds; repetition time (TR)=2.9 seconds; in-plane resolution 0.156×0.156 mm^2) was used to obtain anatomical images. From anterior to posterior sagittal direction, MRI images were taken with a focus of 2.2 to −5.3 mm in the Bregma. The damaged area was scored according to the volume of edema and the area affected, where 1=no damage, 2=mild damage, 3=moderate damage, and 4=severe damage. MRI was used to define brain damage in animals before the long-term behavioral tests.[31] A total of 25 animals (HI/vehicle group, n=12; HI/melatonin group, n=13) were maintained for neurobehavioral tests, which were all scanned using MRI.

Long-Term Neurobehavioral Tests

CatWalk (P46-P48) and novel object recognition (NOR) (P53–P55) as neurobehavioral tests were performed to assess motor and cognitive function, respectively. Three consecutive days were used for the tests, where the first 2 days were designed as the training process and the third day was designed as the experiment day for all neurobehavioral tests.

The CatWalk test was preferred to assess motor function. For the camera and recording, we used the same settings as defined in advance.[32] A maximum run of 5 seconds, with a maximum run variation of <60%, was considered successful. After 2 days of habituation, on the third day, the animals were allowed to run through the CatWalk, and 3 consecutive runs were recorded. Only runs of <5 seconds were recorded. CatWalk XT 10.6 software (Noldus Information Technology, Wageningen, the Netherlands), with the use of automated footprint recognition, was chosen to classify runs and posterior gait and locomotion parameters analysis. Each run was controlled and corrected by a blinded investigator. For the CatWalk analyses, first we classified the paw prints as left front, right front, left hind, and right hind for each run individually in recorded videos. Following that, we continued with the measurement of paw prints (the paw prints are automatically selected by the software), which were toe spread, intermediate toe spread, and print length (data not shown). Run statistics and paw-related parameters were automatically calculated by the software. Gait parameters were exhibited as the median values of 3 runs per animal for each treatment. Three parameters related to gait, step cycle (time [seconds] from when an initial paw contacts the glass surface to the next time the paw comes in contact with the glass surface), stand (contact duration [seconds] of the paw with the glass surface), and swing speed (speed [distance

unit {centimeters per second} of the paw through the swing]) were calculated.

The NOR test was chosen to examine cognitive function (learning ability and memory), which was executed as previously defined.[25] Four 45×45-cm boxes with white walls and a black floor were preferred to perform the NOR. Each rat was habituated in the same empty box for 5 minutes separately, with 2 identical objects positioned in opposite corners during the first 2 days, which were designated as training days. On experiment day (day 3), rats were placed in the same boxes with 2 identical objects for 5 minutes. After a 1-hour pause, 1 of the objects from each box was replaced with a novel object, and the rats were placed in the same boxes for another 5 minutes. Meanwhile, the tests were video recorded and then analyzed using EthoVision XT 17.5 software (Noldus Information Technology). During the analysis, both of the objects (old and new) and the noses of the animals were marked with the help of the software. After the marking process, the noses of the animals were tracked in the videos with the help of the software. Frequency (the number of how many time animals visit the old or novel object) and cumulative duration (time in seconds animals spent with the old or novel object) were analyzed. The ratio of the time (in total) each rat spent scouting 1 of the 2 objects (c) to the time spent scouting the novel object (b) was calculated to ascertain the percentage of time the rat spent scouting the novel object (a): (a=(b/c)×100).

Pharmacodynamic Melatonin Determination

Melatonin was measured in serum/plasma and brain tissue samples from rats using a radioimmunoassay, RK-MEL2, manufactured by NovoLytiX GmbH (Witterswil, Switzerland) according to the instructions for use (version 2022-03-07). Briefly, brain tissue was kept frozen at −80 °C. Approximately 1 g of brain tissue was ground in frozen state with a mortar. Next, 4 mL of ice-cold PBS was added per 1 g of brain tissue to homogenize the crushed brain tissue. The homogenized tissue was incubated for 5 minutes on ice, vortexed vigorously at the highest speed, incubated for another 5 minutes on ice, and then centrifuged for 10 minutes at 10g. The supernatant was transferred into a fresh cryovial and kept at −20 °C for further analysis.

For the blood sample, 50 μL of serum or plasma and the supernatant of brain tissue homogenate, respectively, were extracted over reversed-phase C18 columns. After several washing steps, the melatonin was eluted from the extraction columns with 100% methanol, and the methanol was dried under a stream of nitrogen. The residue containing melatonin was resuspended with 0.5 mL of RK-MEL2 incubation buffer.

Where necessary, the reconstituted samples were further diluted up to 100 000 times with RK-MEL2 incubation buffer to fit into the measuring range of 0.5 to 50 pg/mL of the melatonin radioimmunoassay. Next, 100 μL of iodinated melatonin tracer and 100 μL of melatonin antiserum (G280) were added to 0.4 mL of the diluted samples, calibrators, and controls in duplicates, briefly vortexed, and incubated for 18 to 22 hours at 2 °C to 8 °C. Then, 100 μL of solid-phase bound anti-goat secondary antibody was added, briefly vortexed, and incubated for another 15 minutes at 2 °C to 8 °C. Next, 1 mL of distilled water was added, and the mixtures were centrifuged at 2000g for 2 minutes at 2 °C to 8 °C. The supernatants were aspirated, and the pellets were counted for 2 minutes in a γ-counter, model LB2111 (Berthold Technologies, Zug, Switzerland). The averaged counts per minute of the samples and calibrators were recorded, and a standard curve was generated by the averaged counts per minute of the calibrators applying a 4-parameter logistic algorithm. After intersection of the counts per minute of the samples on the y axis of the graph, the concentrations of the samples could be directly read from the x axis of the graph and finally corrected with the dilution factor applied as described above.

Statistical Analysis

GraphPad Prism 10 software (GraphPad Software, La Jolla, CA) and SPSS Version 27 (IBM, Armonk, NY) were used for all analyses and for data plot construction. All reported data are presented as median and interquartile range (IQR). An ordinary 1-way ANOVA test (using the Tukey multiple comparison test) was performed to analyze protein levels in the AMPK/mTOR/autophagy mechanism at different time points between the different treatment groups. Nonparametric tests (using the Mann–Whitney U test) were performed to analyze the brain area loss, immunohistochemistry, neurobehavioral tests (CatWalk and NOR), and sex comparison data. Linear regression was used to report the effect of sex on brain area loss, weight (P7), weight gain (P14-P7), and AMPK-mTOR levels at P14. Statistical significance was set as $P<0.05$.

RESULTS

Neuroprotective Effects of Melatonin After Hypoxia Ischemia

To determine the effect of melatonin on global brain area loss, we performed hematoxylin and eosin staining 7 days after HI. We observed that melatonin-treated animals showed a significant reduction in global brain area loss compared with the vehicle-treated group (Figures 2A and 2B, 32.93% [HI/vehicle, black triangles] versus 46.79% [HI/melatonin, blue dots]; $P<0.05$).
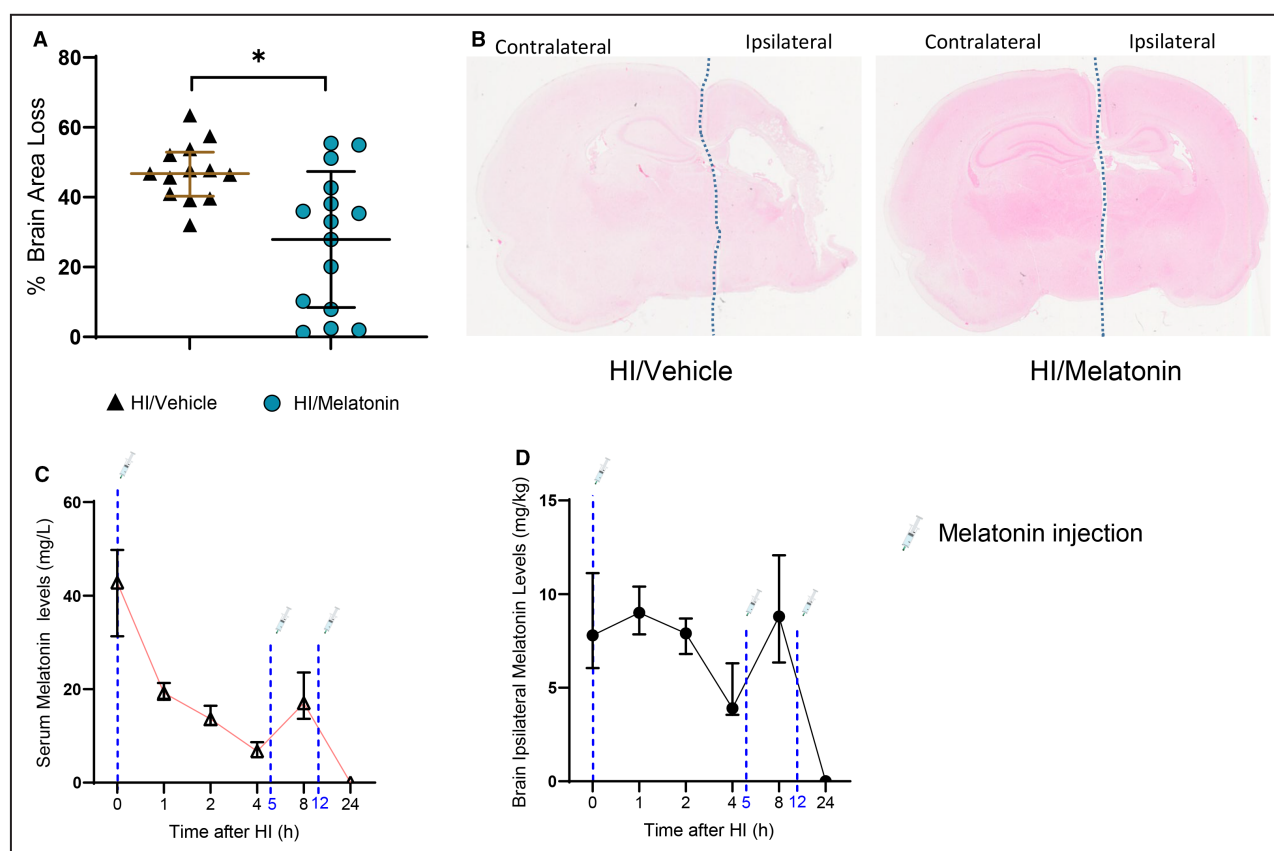
Figure 2.   Brain area loss and pharmacodynamic level data.

A, Graph of global area loss percentages 7 days after HI (median values of global brain area loss in HI/melatonin (n=15) vs HI/vehicle (n=13), 32.93% (blue dots) vs 46.79% [black triangles], respectively). **B**, Representative images of the vehicle solution- and melatonin-treated brains. Nonparametric tests (using the Mann-Whitney *U* test) were performed to analyze the data. **C**, Graph of melatonin's pharmacodynamic levels (milligrams per liter) in the serum after 3 doses of 25 mg/kg melatonin injections. **D**, Graph of melatonin's pharmacodynamic levels (milligrams per kilogram) in the ipsilateral brain hemisphere after 3 doses of 25 mg/kg melatonin injections. HI/melatonin n=4 (0 hours), n=5 (1 hour), n=5 (2 hours), n=5 (4 hours), n=4 (8 hours), n=6 (24 hours). *$P<0.05$. Data in (**A**), (**C**), and (**D**) are presented as the median (IQR). HI indicates hypoxia–ischemia; and IQR, interquartile range.

Our study did not show sex differences for percentage of brain area loss in treatment groups (vehicle and melatonin) in the cortex and hippocampus 5 and 24 hours after HI (Figure S1A). Linear regression for brain area loss, sex, weight, weight gain, and litter showed no significant differences (Table S1).

The pharmacodynamic study showed that a high peak in serum levels of melatonin was observed after the first IP melatonin injection (0 hours after HI), which decreased continuously until the second IP injection 5 hours after HI. A small increase after the second IP injection was observed. However, the levels reached zero 24 hours after HI (Figure 2C). In contrast, melatonin levels in the brain did not reach a peak comparable to what we observed in serum after the first dose and remained stable after a second dose (5 hours after HI). The levels reached zero 24 hours after HI (Figure 2D). There were no significant sex differences in the pharmacodynamic analyses.

Effect of Melatonin on Long-Term Functional Outcomes

To observe the long-term functional outcomes of melatonin, animals were scanned using MRI 7 days after HI treatment with either vehicle or melatonin. Most of the damage was observed between Bregma 2.2 mm and Bregma 5.3 mm (Figures S2A and S2B). The score was based on the size of the edema and the area affected, as previously defined.[25] A total of 25 animals (n=12 HI/vehicle versus n=13 HI/melatonin) were scanned for MRI. The median (range) injury scores for the HI/vehicle and HI/melatonin groups were 3.16 and 3.76 at P14, respectively. We maintained those animals for neurobehavioral tests (CatWalk and NOR) between day 46 and 55.

The CatWalk test was used to determine the motor function of the animals treated with melatonin. In melatonin-treated rats, significant motor improvements

were detected in the neurobehavioral parameters related to the front and hind paws after HI. These improvements were observed for the static parameters of the gait function stand of the 3 limbs (right front, left front, left hind) (Figure 3A, HI/vehicle, black triangles and HI/melatonin, blue dots; $P<0.05$). These significant improvements were also observed for the dynamic parameters of the gait function step cycle and swing speed of the 4 limbs after HI (Figures 3B and 3C, HI/vehicle, black triangles and HI/melatonin, blue dots; $P<0.05$).

Novel object recognition was used to determine the cognitive function of melatonin-treated animals. No significant changes were observed after assessment of cognitive function in animals treated with melatonin (Figures 3D and 3E, HI/vehicle, black triangles and HI/melatonin, blue dots). No sex differences were found in the long-term functional outcomes.

Effects of Melatonin on Inflammation and Oligodendrogenesis After Hypoxia Ischemia

To elucidate the effect of melatonin on inflammation, we performed immunohistochemistry on specific glial cells, such as Iba1 (ionized calcium binding adaptor molecule 1, for microglia cells) and GFAP (for astrocyte cells) in brain tissue 7 days after HI, followed by counting positive cells for Iba1 or measuring the fluorescence intensity for GFAP per area in the cortex, hippocampus, and thalamus (Figure 4A). We did not observe significant changes in the number of Iba1+ or GFAP+ cells in any of the areas analyzed after treatment with melatonin (Figures 4B and 4C, HI/vehicle, black triangles and HI/melatonin, blue dots).

To characterize the effect of melatonin on oligodendrogenesis, CC1 (for mature oligodendrocytes) and Olig2 (for immature oligodendrocytes) staining were performed in brain tissue 7 days after HI, followed by counting positive cells per area in the cortex, hippocampus, thalamus, and amygdala (Figure 5A). We observed a significant increase in CC1+ cells in the cortex and amygdala in the HI/melatonin group compared with the HI/vehicle group (Figure 5B, HI/vehicle, black triangles and HI/melatonin, blue dots; $P<0.05$). In contrast, there was a significant increase in Olig2+ cells in the cortex, hippocampus, thalamus, and amygdala in the HI/melatonin group compared with the HI/vehicle group (Figure 5C, HI/vehicle, black triangles and HI/melatonin, blue dots; $P<0.05$).

Furthermore, MBP was used as a marker of myelination, followed by measuring the MBP fluorescence intensity per area in the corpus callosum, thalamus, and amygdala (Figure 5A). Melatonin-treated brains showed a significant increase in MBP density per area in the corpus callosum, thalamus, and amygdala in

the HI/melatonin group compared with the HI/vehicle group (Figure 5D, HI/vehicle, black triangles and HI/melatonin, blue dots; $P<0.05$).

Melatonin Treatment Regulates the AMPK/mTOR Pathway After Hypoxia Ischemia

To understand the effects of melatonin on the AMPK/mTOR/autophagy mechanism, we isolated cortical and hippocampal areas from the ipsilateral hemisphere and performed Western blotting (Figure 6A and Table 3).

In the cortex, AMPK expression in the sham group was significantly decreased compared with the HI/vehicle group 5 hours after HI (Figures 6B and 6C, sham, white rectangles and HI/vehicle, black triangles; $P<0.05$). In the meantime, there were no significant changes between the sham and HI/melatonin groups in the same area 5 hours after HI (Figures 6B and 6C, sham, white rectangles and HI/melatonin, blue dots). The HI/melatonin group showed a significant decrease compared with the HI/vehicle group 5 hours after HI (Figures 6B and 6C, HI/vehicle, black triangles and HI/melatonin, blue dots; $P<0.05$), whereas no significant changes were observed among the 3 groups 24 hours after HI in the cortex (Figures 6B and 6C, sham, white rectangle; HI/vehicle, black triangles; and HI/melatonin, blue dots).

On the other hand, changes in mTOR levels in the cortex were significant increase in the sham group compared with the HI/vehicle and HI/melatonin groups 5 hours after HI (Figures 6D and 6E, sham, white rectangles; HI/vehicle, black triangles; and HI/melatonin, blue dots; $P<0.05$). A similar pattern was also observed 24 hours after HI, with a significant increase in mTOR levels in the sham group compared with the HI/vehicle and HI/melatonin groups (Figures 6D and 6E, sham, white rectangles; HI/vehicle, black triangles; and HI/melatonin, blue dots; $P<0.05$). Additionally, mTOR levels were also significantly increased in the HI/melatonin group compared with the HI/vehicle group in the same area 24 hours after HI (Figures 6D and 6E, HI/vehicle, black triangles and HI/melatonin, blue dots; $P<0.05$).

In the hippocampus, AMPK level changes in the sham group exhibited a significant increase compared with those in the HI/melatonin group only at 5 and 24 hours after HI. (Figures 6F and 6G, sham, white rectangles and HI/melatonin, blue dots; $P<0.05$), whereas a significant decrease in the HI/melatonin group compared with the HI/vehicle group was observed at 5 and 24 hours after HI in the same area (Figures 6F and 6G, HI/vehicle, black triangles and HI/melatonin, blue dots; $P<0.05$).

In addition, mTOR levels showed no significant changes in the hippocampus between the sham, HI/vehicle, and HI/melatonin groups 5 hours after HI
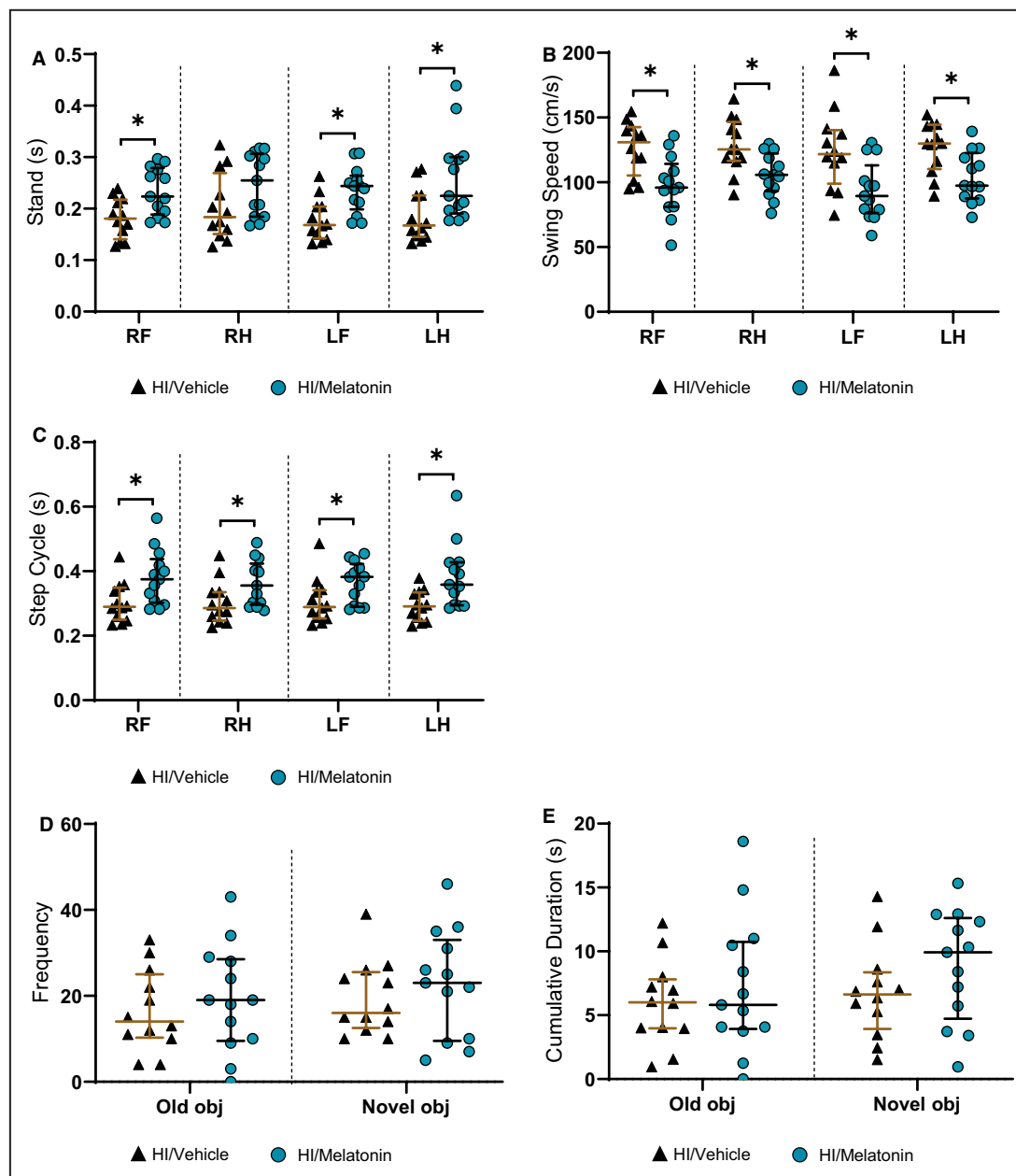
**Figure 3. Graphs of neurobehavioral tests.**
A, Graph of the stand parameter from the CatWalk test analysis. **B**, Graph of the step cycle parameter from the CatWalk test analysis. **C**, Graph of swing speed parameter from the CatWalk test analysis. **D**, Graph of frequency parameter from the NOR test analysis. **E**, Graph of cumulative duration parameter from the NOR test analysis. Nonparametric tests (using the Mann-Whitney U test) were performed to analyze the data. *$P<0.05$. HI/vehicle n=12 (black triangles) vs HI/melatonin n=13 (blue dots). Data are presented as the median (IQR). HI indicates hypoxia–ischemia; IQR, interquartile range; LF, left front; LH, left hind; NOR, novel object recognition; RF, right front; and RH, right hind.

(Figures 6H and 6I, sham, white rectangles; HI/vehicle, black triangles; and HI/melatonin, blue dots). Twenty-four hours after HI, a significant increase in the expression of mTOR was observed in the sham and HI/melatonin groups compared with that in the HI/vehicle group (Figures 6H and 6I, sham, white rectangles; HI/vehicle, black triangles; and HI/melatonin, blue dots; $P<0.05$). Our study did not show sex differences for AMPK and mTOR levels in sham and treatment groups

(vehicle and melatonin) in the cortex and hippocampus 5 and 24 hours after HI (Figures S1 through S1).

Melatonin Regulates the Downstream Translational Factors of mTOR

We examined the activation of 2 major downstream translational factors of mTOR, 4EBP-1 and S6, in the cortex and hippocampus (Figure 7A and Table 3).[9]
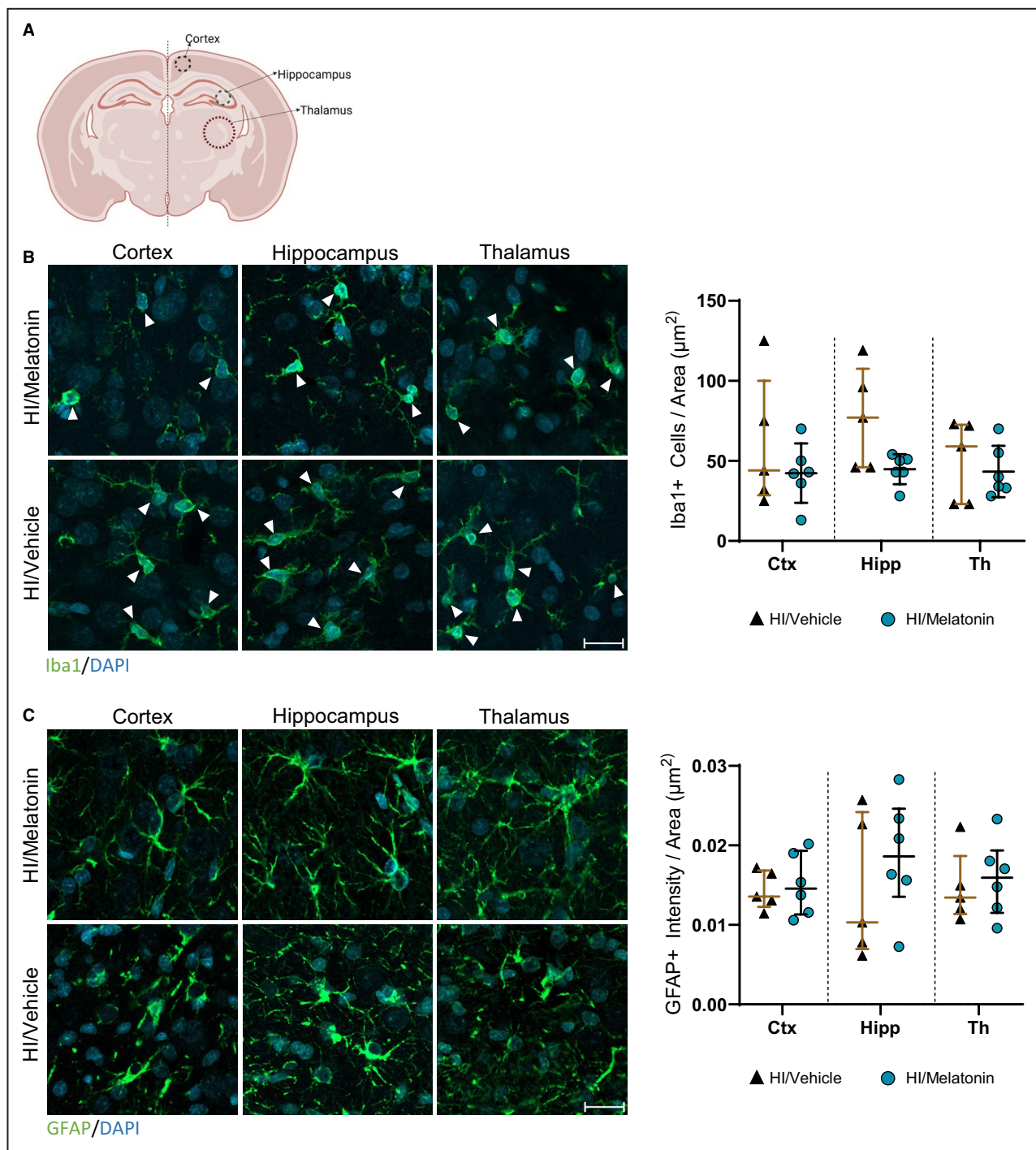
Figure 4.   Immunohistochemistry graphs of Iba1 and GFAP.
A, Representative illustration of the areas analyzed for Iba1 and GFAP staining in the ipsilateral hemisphere. **B**, Representative images of the areas analyzed for Iba1 staining (green) with the nuclear marker DAPI (blue) and quantification of Iba1+ cells per area. **C**, Representative images of the areas analyzed for GFAP staining (green) with the nuclear marker DAPI (blue) and quantification of the fluorescence intensity from GFAP+ per area. Nonparametric tests (using the Mann-Whitney *U* test) were performed to analyze the data. *$P<0.05$. HI/vehicle n=5 vs HI/melatonin n=6. Data are presented as the median (IQR). HI/vehicle (black triangles) vs HI/melatonin (blue dots). Scale bar=20 μm. Image (**A**) was created with Biorender.com. Ctx indicates cortex; HI, hypoxia–ischemia; GFAP, glial fibrillary acidic protein; Hipp, hippocampus; Iba1, ionized calcium binding adaptor molecule 1; IQR, interquartile range; and Th, thalamus.
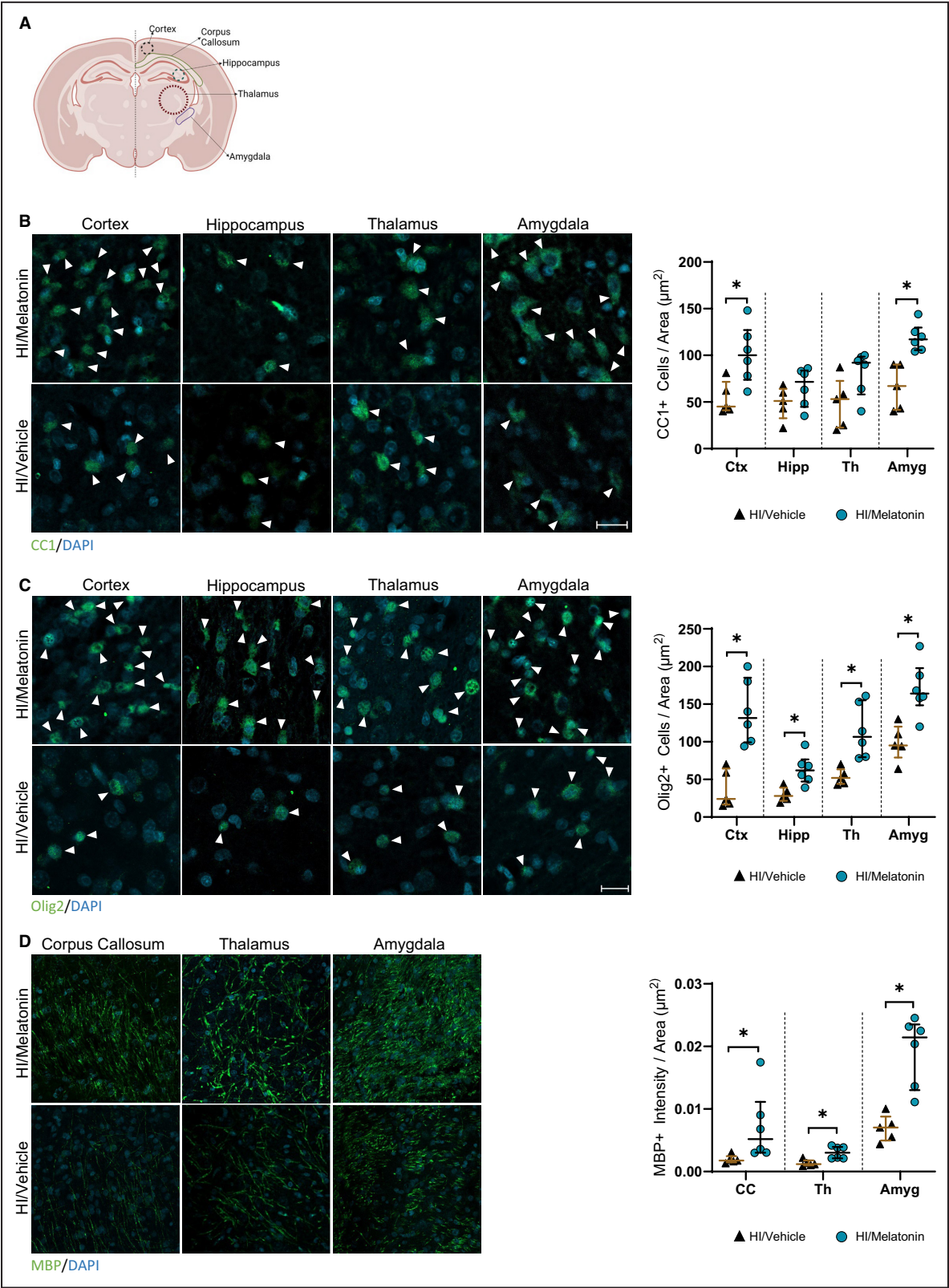
In the cortex, 4EBP-1 expression 5 hours after HI was characterized by a significant increase in the HI/melatonin group compared with the HI/vehicle group (Figures 7B and 7C, HI/vehicle, black triangles and HI/melatonin, blue dots; $P < 0.05$). Twenty-four hours after HI, 4EBP-1 levels in the sham group expressed a significant decrease compared with the HI/melatonin group in the cortex (Figures 7B and 7C, sham,

Figure 5. **Immunohistochemistry graphs of Olig2, CC1, and MBP.**
A, Representative illustration of the areas analyzed for CC1, Olig2, and MBP staining in the ipsilateral hemisphere. **B**, Representative images of the areas analyzed for CC1 staining (green) with the nuclear marker DAPI (blue) and quantification of CC1+ cells per area. **C**, Representative images of the areas analyzed by Olig2 staining (green) with the nuclear marker DAPI (blue) and quantification of Olig2+ cells per area. **D**, Representative pictures of the areas analyzed for MBP staining (green) with the nuclear marker DAPI (blue) and quantification of MBP+ intensity per area. Nonparametric tests (using the Mann-Whitney U test) were performed to analyze the data. *$P<0.05$. HI/vehicle n=5 vs HI/melatonin n=6. Data are presented as the median (IQR). HI/vehicle (black triangles) vs HI/melatonin (blue dots). Scale bar=20 μm for CC1 and Olig2 and 50 μm for MBP. Image (**A**) created with Biorender.com. Amyg indicates amygdala; CC, corpus callosum; CC1, adenomatous polyposis coli APC; Ctx, cortex; HI, hypoxia–ischemia; Hipp, hippocampus; IQR, interquartile range; MBP, myelin basic protein; Olig2, oligodendrocyte-2; and Th, thalamus.

white rectangles and HI/melatonin, blue dots; $P<0.05$), whereas levels significantly increased in the HI/melatonin group compared with the HI/vehicle group (Figures 7B and 7C, HI/vehicle, black triangles and HI/melatonin, blue dots; $P<0.05$).

S6 levels showed a significant increase in the sham group compared with the HI/vehicle and HI/melatonin groups 5 hours after HI in the cortex (Figures 7D and 7E, sham, white rectangles; HI/vehicle, black triangles; and HI/melatonin, blue dots; $P<0.05$), whereas its levels in the HI/melatonin group also expressed a significant increase compared with the HI/vehicle group 5 hours after HI in the same area (Figures 7D and 7E, HI/vehicle, black triangles and HI/melatonin, blue dots; $P<0.05$). On the other hand, a significant decrease was observed in the sham group compared with the HI/melatonin group at 24 hours after HI in the same area (Figures 7D and 7E, sham, white rectangles and HI/melatonin, blue dots; $P<0.05$). S6 levels in the HI/melatonin group expressed a significant increase compared with the HI/vehicle group at same time point in the cortex (Figures 7D and 7E, HI/vehicle, black triangles and HI/melatonin, blue dots; $P<0.05$).

In the hippocampus, the expression levels of 4EBP-1 5 hours after HI showed a significant increase in the HI/melatonin group compared with the HI/vehicle group (Figures 7F and 7G, HI/vehicle, black triangles and HI/melatonin, blue dots; $P<0.05$). Twenty-four hours after HI, a significant increase was detected in the sham group compared with the HI/vehicle group (Figures 7F and 7G, sham, white rectangles and HI/vehicle, black triangles; $P<0.05$). However, there was no significant change between sham and HI/melatonin groups at the same time point in the hippocampus (Figures 7F and 7G, sham, white rectangles and HI/melatonin, blue dots). In the meantime, a significant increase was detected in the HI/melatonin group compared with the HI/vehicle group in the same area 24 hours after HI (Figures 7F and 7G, HI/vehicle-black triangles and HI/melatonin, blue dots; $P<0.05$).

In addition, S6 showed a significant decrease in the sham group compared with the HI/melatonin group 5 hours after HI in the hippocampus (Figures 7H and 7I, sham, white rectangles and HI/melatonin, blue dots; $P<0.05$). A similar change of pattern in S6 levels in the

sham group at 5 hours after HI was also observed at 24 hours after HI compared with the HI/vehicle and HI/melatonin groups in the same region (Figures 7H and 7I, sham, white rectangles; HI/vehicle, black triangles; and HI/melatonin, blue dots; $P<0.05$). The HI/melatonin group expressed a significant increase in the S6 levels compared with the HI/vehicle group 24 hours after HI in the hippocampus (Figures 7H and 7I, HI/vehicle, black triangles and HI/melatonin, blue dots; $P<0.05$).

## Melatonin Regulates the Transcriptional Factors

Between several transcriptional factors regulated by mTOR, we decided to analyze HIF1α and NF-κβ because of their roles in hypoxia ischemia (Figure 8A and Table 3).[19,33,34]

In the cortex, HIF1a expressions showed a significant increase in the sham group compared with the HI/vehicle group at 5 and 24 hours after HI (Figures 8B and 8C, sham, white rectangles and HI/vehicle, black triangles; $P<0.05$). Additionally, its levels increased also in the HI/melatonin group compared with the HI/vehicle group 5 and 24 hours after HI in the same area (Figures 8B and 8C, HI/vehicle, black triangles and HI/melatonin, blue dots; $P<0.05$).

NF-κβ levels increased significantly in the HI/melatonin group compared with the HI/vehicle and sham groups 5 hours after HI in the cortex (Figures 8D and 8E, sham, white rectangles; HI/vehicle, black triangles; and HI/melatonin, blue dots; $P<0.05$). Twenty-four hours after HI, a significant decrease in its levels occurred in the sham group compared with the HI/vehicle group in the cortex (Figures 8D and 8E, sham, white rectangles and HI/vehicle, black triangles; $P<0.05$). Additionally, its levels significantly decreased in the HI/melatonin group compared with the sham and HI/vehicle groups at the same time point in the cortex (Figures 8D and 8E, sham, white rectangles; HI/vehicle, black triangles; and HI/melatonin, blue dots; *$P<0.05$).

In the hippocampus, HIF1α levels were not significantly different among the sham, HI/vehicle, and HI/melatonin groups at 5 hours after HI (Figures 8F and 8G, sham, white rectangles; HI/vehicle, black triangles; and HI/melatonin, blue dots). A significant increase was
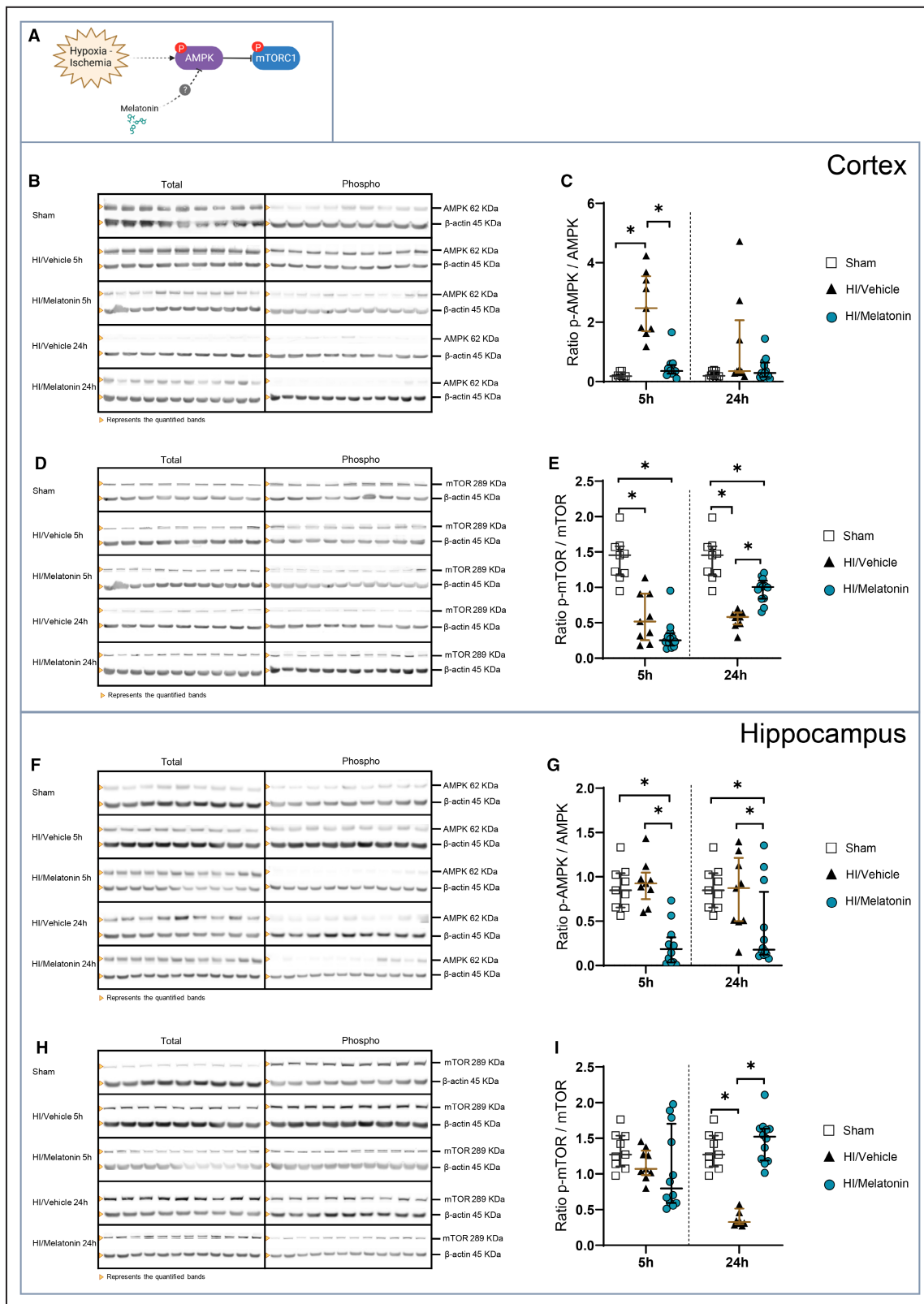
observed in the sham group compared with the HI/vehicle and HI/melatonin groups in the same brain region at 24 hours after HI, which are all changes detected at this time point (Figures 8F and 8G, sham, white rectangles; HI/vehicle, black triangles; and HI/melatonin, blue dots; *P*<0.05).

Figure 6. AMPK and mTOR regulations on treatment.
A, Representative illustration of HI insult, AMPK, and mTORC1 relationship. **B,** Representative Western blot images of total and phospho AMPK bands and β-actin bands in the cortex at 5 and 24 hours after HI. **C**, Plot of the ratio of p-AMPK to AMPK in the cortex at 5 and 24 hours after HI. β-actin was used for loading control. **D**, Representative Western blot images of total and phospho mTOR bands and β-actin bands in the cortex at 5 and 24 hours after HI. **E**, Plot of the ratio of p-mTOR to mTOR in the cortex at 5 and 24 hours after HI. β-actin was used for loading control. **F**, Representative Western blot images of total and phospho AMPK bands and β-actin bands in the hippocampus at 5 and 24 hours after HI. **G**, Plot of the ratio of p-AMPK to AMPK in the hippocampus at 5 and 24 hours after HI. β-actin was used for loading control. **H**, Representative Western blot images of total and phospho mTOR bands and β-actin bands in the hippocampus at 5 and 24 hours after HI. **I**, Plot of the ratio of p-mTOR to mTOR in the hippocampus at 5 and 24 hours after HI. β-actin was used for loading control. Ordinary 1-way ANOVA tests (using the Tukey multiple comparison test) were performed to analyze the data. *$P<0.05$. Sham n=9 vs HI/vehicle n=9 (5 hours) and n=9 (24 hours) vs HI/melatonin n=12 (5 hours) and n=12 (24 hours). Data are presented as the median (IQR). Sham (white rectangles), HI/vehicle (black dots), HI/melatonin (blue dots). Image (**A**) created with Biorender.com. AMPK indicates AMPK-activated protein kinase; HI, hypoxia–ischemia; IQR, interquartile range; mTOR, mammalian target of rapamycin; mTORC1, mammalian target of rapamycin complex 1; p-AMPK, phosphorylated AMP-activated protein kinase; and p-mTOR, phosphorylated mammalian target of rapamycin.

In addition, NF-κβ expression showed a significant decrease in the HI/melatonin group compared with the sham and HI/vehicle groups 5 hours after HI in the hippocampus (Figures 8H and 8I, sham, white rectangles and HI/melatonin, blue dots; $P<0.05$). Twenty-four hours after HI, a significant decrease was detected in NF-κβ levels in the sham group compared with the HI/vehicle group in the hippocampus (Figures 8H and 8I, sham, white rectangles and HI/vehicle, black triangles; $P<0.05$). Nonsignificant changes in NF-κβ levels were observed between the sham and HI/melatonin groups 24 hours after HI in the same region (Figures 8H and 8I, sham, white rectangles and HI/melatonin, blue dots). In the HI/melatonin group, a significant decrease occurred in NF-κβ levels compared with the HI/vehicle group in the hippocampus 24 hours after HI (Figures 8H and 8I, HI/vehicle, black triangles and HI/melatonin, blue dots; $P<0.05$).

Melatonin Inhibits the Autophagy Related Factor ULK-1/P62/LC3

To elucidate the effect of melatonin on autophagy, we first characterized the expression levels of ULK-1 by measuring changes in the serine 555 and serine 757 subunits (Figure 9A and Table 4).

In the cortex, ULK-1 serine 555 levels were significantly higher in the sham group compared with the HI/vehicle group 5 hours after HI (Figures 9B and 9C, sham, white rectangles and HI/vehicle, black triangles; $P<0.05$). Its levels in the HI/melatonin group were significantly increased compared with the HI/vehicle group 5 hours after HI in the same area (Figures 9B and 9C, HI/vehicle, black triangles and HI/melatonin, blue dots; $P<0.05$). Twenty-four hours after HI, ULK-1 serine 555 levels decreased significantly in the sham group compared with the HI/vehicle and HI/melatonin groups in the cortex (Figures 9B and 9C, sham, white rectangles; HI/vehicle, black triangles; and HI/melatonin, blue dots; $P<0.05$). Additionally, its levels also decreased in the HI/melatonin group compared with the HI/vehicle

group at the same time point in the cortex (Figures 9B and 9C, HI/vehicle, black triangles and HI/melatonin, blue dots; $P<0.05$).

Meanwhile, ULK-1 serine 757 levels in the sham group were significantly higher than those in the HI/vehicle and HI/melatonin groups 5 hours after HI in the cortex (Figures 9D and 9E, sham, white rectangles; HI/vehicle, black triangles; and HI/melatonin, blue dots; $P<0.05$). Significant decreases were also appointed in ULK-1 serine 757 levels in the HI/melatonin group compared with the HI/vehicle group 5 and 24 hours after HI in the cortex (Figures 9D and 9E, HI/vehicle, black triangles and HI/melatonin, blue dots; $P<0.05$). Meanwhile, ULK-1 serine 757 expression in the sham group exhibited a significant decrease and a significant increase compared with the HI/vehicle and HI/melatonin groups, respectively, in the cortex 24 hours after HI (Figures 9D and 9E, sham, white rectangles; HI/vehicle, black triangles; and HI/melatonin, blue dots; $P<0.05$).

In the hippocampus, ULK-1 serine 555 levels were changed nonsignificantly between the sham and HI/vehicle groups 5 hours after HI (Figures 9F and 9G, sham, white rectangles and HI/vehicle, black triangles), whereas its levels decreased significantly in the sham group compared with the HI/melatonin group 5 and 24 hours after HI in the same area (Figures 9F and 9G, sham, white rectangles and HI/melatonin, blue dots; $P<0.05$). In the HI/melatonin group, ULK-1 serine 555 levels presented a significant increase compared with the HI/vehicle group 5 and 24 hours after HI in the hippocampus (Figures 9F and 9G, HI/vehicle, black triangles and HI/melatonin, blue dots; $P<0.05$). In addition, its levels in the sham group decreased significantly compared with the HI/vehicle group at the same time point in the same area (Figures 9F and 9G, sham, white rectangles and HI/vehicle, black triangles; $P<0.05$).

ULK-1 serine 757 levels also exhibited a significant increase in the sham group compared with the HI/vehicle and HI/melatonin groups at 5 and 24 hours after HI in the hippocampus (Figures 9H and 9I, sham, white

Table 3. AMPK/mTOR Pathway Protein Expressions

Protein	Time point (h)	Condition	Cortex		Hippocampus	
			Compared with sham	Compared with HI/veh	Compared with sham	Compared with HI/veh
AMPK	5	HI/veh	↑	…	…	…
		HI/mel	…	↓	↓	↓
	24	HI/veh	…	…	…	…
		HI/mel	…	…	↓	↓
mTOR	5	HI/veh	↓	…	…	…
		HI/mel	↓	…	…	…
	24	HI/veh	↓	…	↓	…
		HI/mel	↓	↑	…	↑
4EBP-1	5	HI/veh	…	…	…	…
		HI/mel	…	↑	…	↑
	24	HI/veh		…	↓	…
		HI/mel	↑	↑	…	↑
S6	5	HI/veh	↓	…	…	…
		HI/mel	↓	↑	↑	…
	24	HI/veh	…	…	…	…
		HI/mel	↑	↑	↑	↑
HIF1α	5	HI/veh	↓	…	…	
		HI/mel	…	↑	…	…
	24	HI/veh	↓	…	↓	…
		HI/mel	…	↑	↓	…
NF-κβ	5	HI/veh	…	…	…	…
		HI/mel	↑	↑	↓	↓
	24	HI/veh	↑	…	↑	…
		HI/mel	↓	↓	…	↓

↑↓ = Significant change.

4EBP-1 indicates eukaryotic translation initiation factor 4E (eIF4E)-binding protein 1; AMPK, AMP-activated protein kinase; HIF1α, hypoxia-inducible factor 1α; HI/mel, hypoxia–ischemia melatonin solution-treated group; HI/veh, hypoxia–ischemia vehicle solution-treated group; mTOR, mammalian target of rapamycin; and NF-κβ, nuclear factor-κβ.

rectangles; HI/vehicle, black triangles; and HI/melatonin, blue dots; *P*<0.05). Its levels in the HI/melatonin group were increased significantly compared with the HI/vehicle group at 5 hours after HI in the hippocampus (Figures 9H and 9I, HI/vehicle, black triangles and HI/melatonin, blue dots; *P*<0.05) and expressed nonsignificant changes compared with the HI/vehicle group at 24 hours after HI in the same brain region (Figures 9H and 9I, HI/vehicle, black triangles and HI/melatonin, blue dots; *P*<0.05).

Autophagy-related biomarkers were then followed by analyses of LC3 and p62 (Figure 9A and Table 4).

In the cortex, LC3 levels in the sham group were altered compared with the HI/melatonin group, which
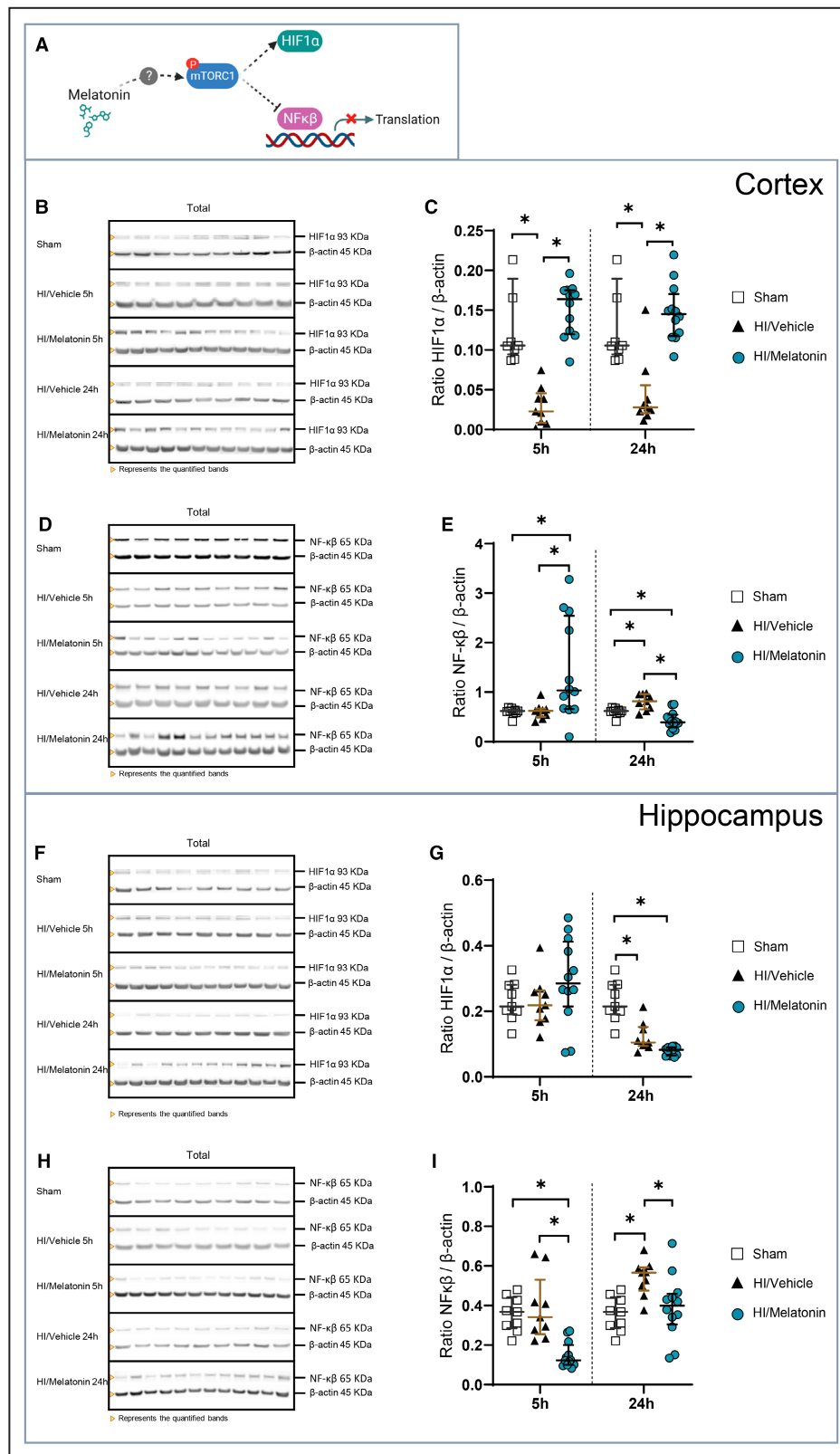
Figure 7. 4EBP-1 and S6 regulations on treatment.
A, Representative illustration of translation factors 4EBP-1 and S6. **B**, Representative Western blot images of total and phospho 4EBP-1 bands and β-actin bands in the cortex at 5 and 24 hours after HI. **C**, Plot of the ratio of p4EBP-1 to 4EBP-1 in the cortex at 5 and 24 hours after HI. β-actin was used for loading control. **D**, Representative Western blot images of total and phospho S6 bands and β-actin bands in the cortex at 5 and 24 hours after HI. **E**, Plot of the ratio of p-S6 to S6 in the cortex at 5 and 24 hours after HI. β-actin was used for loading control. **F**, Representative Western blot images of total and phospho 4EBP-1 bands and β-actin bands in the hippocampus at 5 and 24 hours after HI. **G**, Plot of the ratio of p4EBP-1 to 4EBP-1 in the hippocampus at 5 and 24 hours after HI. β-Actin used for loading control. **H**, Representative Western blot images of total and phospho S6 bands and β-actin bands in the hippocampus at 5 and 24 hours after HI. **I**, Plot of the ratio of p-S6 to S6 in the hippocampus at 5 and 24 hours after HI. β-actin was used for loading control. Ordinary 1-way ANOVA tests (using the Tukey multiple comparison test) were performed to analyze the data. *P<0.05. Sham n=9 vs HI/vehicle n=9 (5 hours) and n=9 (24 hours) vs HI/melatonin n=12 (5 hours) and n=12 (24 hours). Data are presented as the median (IQR). Sham (white rectangles), HI/vehicle (black dots), HI/melatonin (blue dots). Image (**A**) created with Biorender.com. 4EBP-1 indicates eukaryotic translation initiation factor 4E (eIF4E)-binding protein 1; HI, hypoxia–ischemia; IQR, interquartile range; mTORC1, mammalian target of rapamycin complex 1; p4EBP-1, phosphorylated eukaryotic translation initiation factor 4E (eIF4E)-binding protein 1; and p-S6, phosphorylated S6.

are characterized by significant increases in the cortex 5 and 24 hours after HI (Figures 10A and 10B, sham, white rectangles and HI/melatonin, blue dots; P<0.05). In contrast, significant decreases were observed in the HI/melatonin group compared with the

HI/vehicle group at 5 and 24 hours after HI in the cortex (Figures 10A and 10B, HI/vehicle, black triangles and HI/melatonin, blue dots; P<0.05). Additionally, its levels in the sham group decreased significantly compared with the HI/vehicle group 24 hours after HI in the cortex
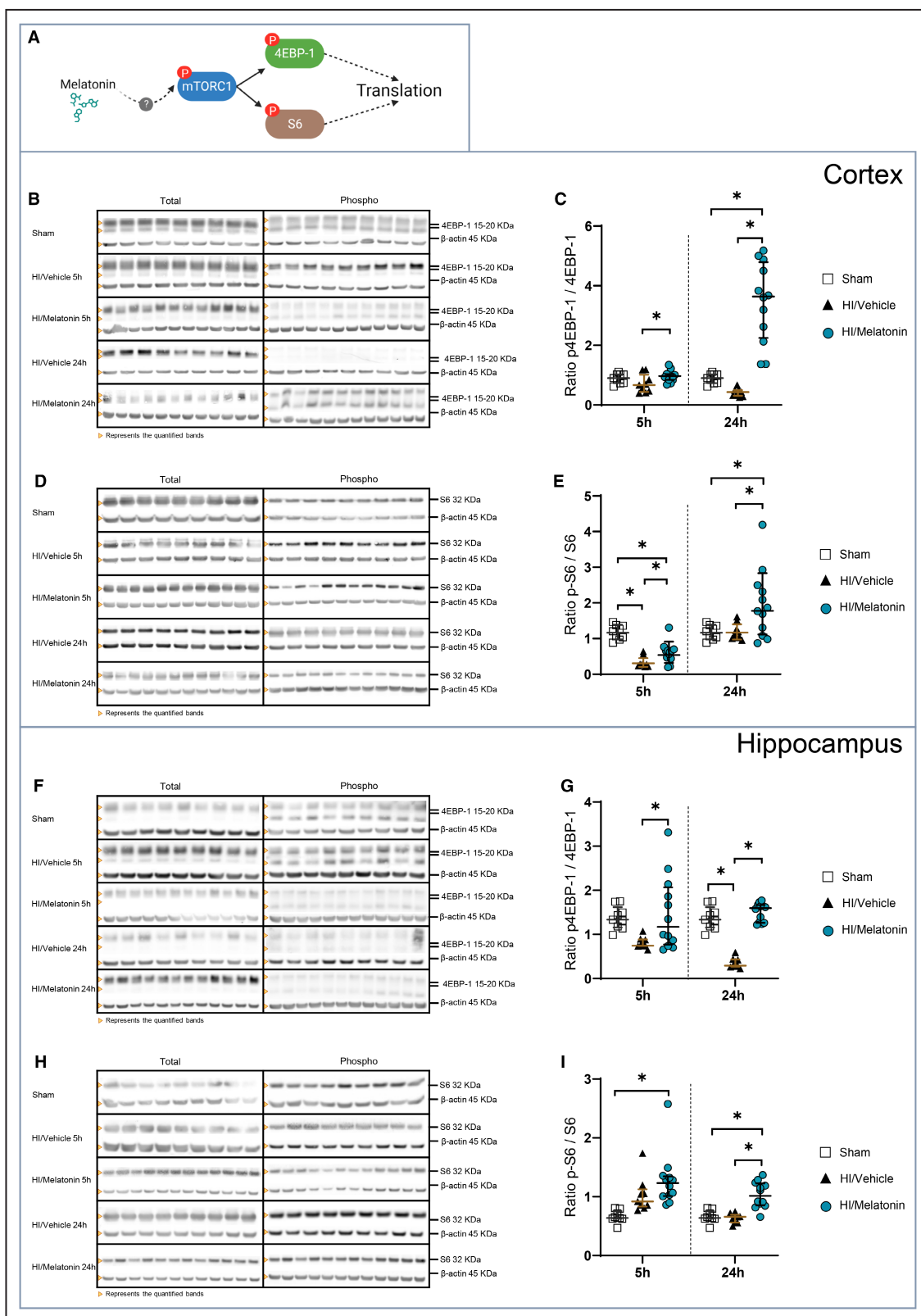
(Figures 10A and 10B, sham, white rectangles and HI/vehicle, black triangles; $P<0.05$).

On the other hand, p62 levels in the cortex did not show a significant difference between the sham, HI/vehicle, and HI/melatonin groups 5 hours after HI (Figures 10C and 10D, sham, white rectangles; HI/vehicle, black triangles; and HI/melatonin, blue dots). Concurrently, p62 levels were significantly increased in the sham group compared

Figure 8. HIF1α and NF-κβ regulations on treatment.
A, Representative illustration of the translational factors HIF1α and NF-κβ. **B**, Representative Western blot images of total HIF1α bands and β-actin bands in the cortex at 5 and 24 hours after HI. **C**, Plot of the ratio of HIF1α to β-actin in the cortex at 5 and 24 hours after HI. β-actin used for loading control. **D**, Representative Western blot images of total NF-κβ bands and β-actin bands in the cortex at 5 and 24 hours after HI. **E**, Plot of the ratio of NF-κβ to β-actin in the cortex at 5 and 24 hours after HI. β-actin was used for loading control. **F**, Representative Western blot images of total HIF1α bands and β-actin bands in the hippocampus at 5 and 24 hours after HI. **G**, Plot of the ratio of HIF1α to β-actin in the hippocampus at 5 and 24 hours after HI. β-actin was used for loading control. **H**, Representative Western blot images of total NF-κβ bands and β-actin bands in the hippocampus at 5 and 24 hours after HI. **I**, Plot of the ratio of NF-κβ to β-actin in the hippocampus at 5 and 24 hours after HI. β-actin was used for loading control. Ordinary 1-way ANOVA tests (using the Tukey multiple comparison test) were performed to analyze the data. *$P<0.05$. Sham n=9 vs HI/vehicle n=9 (5 hours) and n=9 (24 hours) vs HI/melatonin n=12 (5 hours) and n=12 (24 hours). Data are presented as the median (IQR). Sham (white rectangles), HI/vehicle (black dots), and HI/melatonin (blue dots). Image (**A**) created with Biorender.com. HI indicates hypoxia–ischemia; HIF1α, hypoxia-inducible factor 1α; IQR, interquartile range; mTORC1, mammalian target of rapamycin complex 1; and NF-κβ, nuclear factor-κβ.

with the HI/melatonin group at 24 hours after HI in the cortex (Figures 10C and 10D, sham, white rectangles and HI/melatonin, blue dots; $P<0.05$). A significant decrease in p62 expression occurred in the HI/melatonin group compared with that in the HI/vehicle group 24 hours after HI in the cortex (Figures 10C and 10D, HI/vehicle, black triangles and HI/melatonin, blue dots; $P<0.05$).

In the hippocampus, LC3 levels exhibited no significant changes among the sham, HI/vehicle, and HI/melatonin groups 5 hours after HI (Figures 10E and 10F, Sham, white rectangles; HI/vehicle, black triangles; and HI/melatonin, blue dots). Furthermore, its levels in the sham group 24 hours after the HI/vehicle group exhibited a significant change compared with the HI/melatonin group only, which is characterized by a significant increase in the same area (Figures 10E and 10F, sham, white rectangles; HI/vehicle, black triangles; and HI/melatonin, blue dots; $P<0.05$). Additionally, its levels expressed a significant decrease in the HI/melatonin group compared with the HI/vehicle group 24 hours after HI (Figures 10E and 10F, HI/vehicle, black triangles and HI/melatonin, blue dots; $P<0.05$).

Concurrently, p62 levels were presented significant increases in the sham group compared with the HI/melatonin group 5 and 24 hours after HI in the same brain region (Figures 10G and 10H, sham, white rectangles and HI/melatonin, blue dots; $P<0.05$). Its levels significantly decreased in the HI/melatonin group compared with the HI/vehicle group 5 and 24 hours after HI in the hippocampus (Figures 10G and 10H, HI/vehicle, black triangles and HI/melatonin, blue dots; $P<0.05$). In addition, a significant increase was observed in the sham group compared with the HI/vehicle group 24 hours after HI (Figures 10G and 10H, sham, white rectangles and HI/vehicle, black triangles; $P<0.05$).

DISCUSSION

In this study, we demonstrated the neuroprotective effects of melatonin in a rat model of neonatal hypoxic–ischemic brain injury. We also validated that melatonin at a concentration of 25 mg/kg administered after HI reduced global brain damage 7 days after HI and improved behavioral parameters related to motor function 41 days after HI. Our results demonstrated that the neuroprotective effects of melatonin are not related to changes in inflammatory responses after HI but have a clear effect on oligodendrogenesis and myelination. We demonstrated that the neuroprotective effects of melatonin are regulated by the AMPK/mTOR/autophagy pathway in a time-dependent and specific brain area-dependent manner.

Lack of oxygen and blood supply to the brain during neonatal HI is responsible for long-lasting disabilities.[35–37] TH is the currently used treatment option.[4] However, its effectiveness is limited among neonates,[38–40] and particularly in LMICs, many neonates do not benefit from TH.[6] Owing to these limitations and restrictions, the search for new treatment options has emerged.

Melatonin, an indolamine hormone, is mainly synthesized by the pineal gland[41] and is a potential candidate for neonatal HIE cases. Its anti-inflammatory and antioxidant effects in the neonatal HIE rat model[19] and its antiapoptotic effect in an adult mouse model of focal ischemia[42] have been previously demonstrated. It has also been shown that low-dose maternal melatonin treatment can improve brain functions (electroencephalogram recovery, delayed onset of seizures) and improve the survival of oligodendrocytes in a preterm fetal sheep HIE model[43]; melatonin treatment in combination with TH can improve electroencephalogram recovery, reduce TUNEL (terminal deoxynucleotidyl transferase dUTP nick end labeling)-positive cells, and increase the number of oligodendrocytes in a neonatal HIE piglet model.[28,44] However, in addition to its beneficial effects, it also has shortcomings, such as degrading in the presence of ultraviolet light (ultraviolet light-A and ultraviolet light-B), being metabolized in the liver and excreted in urine, thus affecting its elimination in liver and kidney diseases, and requiring excipients or solubility enhancers because of its poor water solubility.[22]

Ethanol is one of the most preferred excipient agents in preclinical models.[28,43,45] However, it has been previously shown that ethanol can affect cellular death in the brain of a preterm fetal sheep model.[43] To avoid this
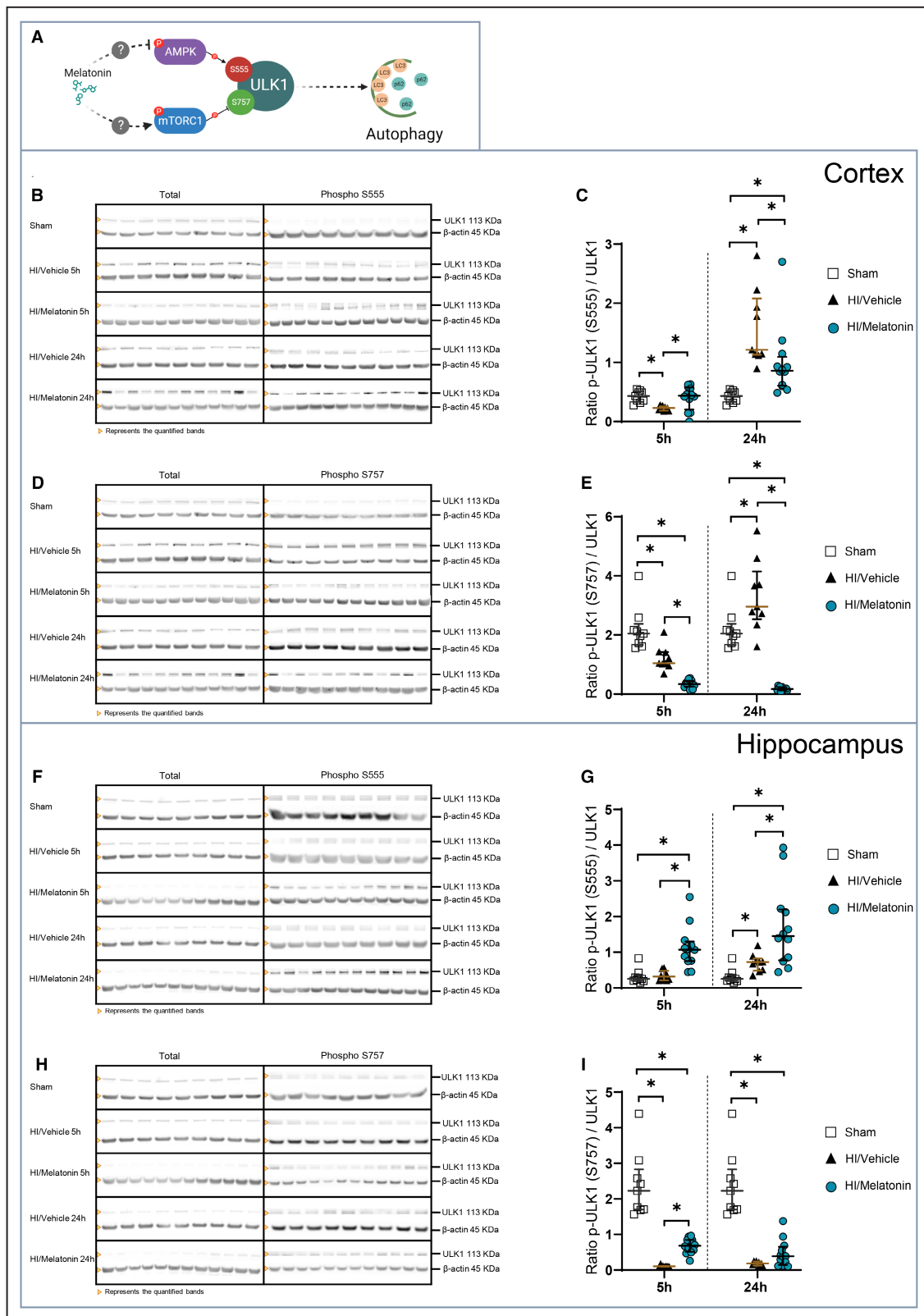
characteristic of ethanol, we used an ethanol-free solution (CHIESI Farmaceutici, Parma, Italy) as an excipient and vehicle solution.

Another limitation of melatonin as a neuroprotective agent is that its effects are dose dependent and time critical.[46] Our results also demonstrated that melatonin

Figure 9. Regulation of the S555 and S757 subunits of ULK-1 on treatment.

A, Representative illustration of the effects of AMPK/mTOR on the S555 and S757 subunits of ULK-1. **B**, Representative Western blot images of ULK-1 and p-ULK-1 serine 555 bands and β-actin bands in the cortex at 5 and 24 hours after HI. **C**, Plot of the ratio of p-ULK-1 serine 555 to ULK-1 in the cortex at 5 and 24 hours after HI. β-actin was used for loading control. **D**, Representative Western blot images of ULK-1 and p-ULK-1 serine 757 bands and β-actin bands in the cortex at 5 and 24 hours after HI. **E**, Plot of the ratio of p-ULK-1 serine 757 to ULK-1 in the cortex at 5 and 24 hours after HI. β-actin was used for loading control. **F**, Representative Western blot images of ULK-1 and p-ULK-1 serine 555 bands and β-actin bands in the hippocampus at 5 and 24 hours after HI. **G**, Plot of the ratio of p-ULK-1 serine 555 to ULK-1 in the hippocampus at 5 and 24 hours after HI. β-actin was used for loading control. **H**, Representative Western blot images of ULK-1 and p-ULK-1 serine 757 bands and β-actin bands in the hippocampus at 5 and 24 hours after HI. **I**, Plot of the ratio of p-ULK-1 serine 7575 to ULK-1 in the hippocampus at 5 and 24 hours after HI. β-actin was used for loading control. Ordinary 1-way ANOVA tests (using the Tukey multiple comparison test) were performed to analyze the data. *$P<0.05$. Sham n=9 vs HI/vehicle n=9 (5 hours) and n=9 (24 hours) vs HI/melatonin n=12 (5 hours) and n=12 (24 hours). Data are presented as the median (IQR). Sham (white rectangles), HI/vehicle (black dots), and HI/melatonin (blue dots). Image (**A**) created with Biorender.com. AMPK indicates AMP-activated protein kinase; HI, hypoxia–ischemia; IQR, interquartile range; LC3, microtubule-associated proteins 1A/1B light chain 3B; mTOR, mammalian target of rapamycin; mTORC1, mammalian target of rapamycin complex 1; p-ULK-1 (S555), phosphorylated ULK-1 serine 555; P62, Protein 62; p-ULK-1 (S757), phosphorylated ULK-1 serine 757; and ULK-1, uncoordinated-51-like kinase 1.

requires several dose applications to achieve a certain effect due to its pharmacodynamics. It has been demonstrated that melatonin treatment directly after HI, with a subsequent dose at 6 and 25 hours after HI, protects against early injury and provides transient and subtle neuroprotection, but is not sufficient to mitigate long-term brain injury.[47] Considering this and the short half-life of melatonin, which is approximately 20 minutes with a bioavailability of 75%,[48] in the present study, we decided to use a regime dose with the first dose immediately after HI, following with a second dose immediately after normothermia treatment (5 hours after HI) so as not to disturb the animals once they are relocated with the dams, followed by consecutive doses every 12 hours for an extension of 48 hours after HI. Considering this range, we hypothesize extended long-term brain neuroprotection as observed in our results, particularly in our behavioral test.

The sensation of stress at the molecular level is one of the key factors in the response to stress conditions,[49] and it is important to understand these mechanisms to underlie the neuroprotective effect of compounds in the treatment of HIE. AMPK activation plays an important role in brain development, and its expression is extremely high, particularly in the cortical and hippocampal areas of the brain.[50] It can sense energy changes in cells and restore cellular energy balance[50] by promoting alternative catabolic reactions and regulating anabolic activities to maintain energy levels for essential cell survival.[9] mTOR regulates many cellular mechanisms such as cell survival, autophagy, and the cell cycle.[9,10] It has been previously shown that AMPK activation may inhibit the phosphorylation of mTOR in cellular level.[51] mTOR also plays a role in the regulation of many downstream substrates, such as 4EBP-1 and S6, autophagosome markers, such as ULK-1, LC3, and p62, and some transcription factors such as NF-κβ and HIF1α.[52–55] In our study, we demonstrated that melatonin treatment regulated AMPK and mTOR expression shortly after HI injury in the brain.

We found that melatonin regulated 4EBP-1 and S6 expression via mTORC1 in our neonatal HI rat model. 4EBP-1 and S6 play key roles in cap-dependent translation.[55] Activation of 4EBP-1 is possible via mTOR, and this effect can be reversed by rapamycin, a specific inhibitor of mTOR, in an adult mouse model of aging.[55] Activation of mTORC1 increases the expression of S6K, which subsequently activates S6 and has been shown to affect cap-dependent translation as well as neuroinflammation in a neonatal HI rat model.[56]

To date, the majority of research investigating the connection between the AMPK/mTOR pathway (along with its downstream substrates) and the HI model has been conducted using different adaptations of the neonatal HI Vannucci model[57–59] or in adult models simulating stroke or other instances of brain damage.[60,61] However, these results cannot be easily adapted to the neonatal brain because of the differences between adult and neonatal brains. Therefore, more in-depth investigations are needed to understand the correlation between the mechanisms involved in maintaining cellular homeostasis after stress, starvation, and neonatal HI.

Activation of mTORC1 also regulates HIF1α and NF-κβ.[17,18] It has been reported that HIF1α levels can increase more under hypoxic conditions than under HI conditions in a neonatal HI rat model,[33] and mTOR plays an important role in this regulation.[53] Our data suggest that HIF1α expression can be positively regulated by mTOR after melatonin treatment in neonatal HI rat brains. In contrast, mTOR activity can negatively regulate NF-κβ at the cellular level.[18] It has been previously shown that melatonin treatment in a neonatal HIE rat model or neonatal piglet model of HIE shows anti-inflammatory features, probably due to the reduction of transcription factors such as NF-κβ.[19,28]

There are some limitations to our study. First, we did not directly measure melatonin receptor activation in our study. Neuroprotection by melatonin has been demonstrated to be mediated via receptor and nonreceptor

Table 4.   **Autophagy Marker Expressions**

Protein	Time point (h)	Condition	Cortex Compared with sham	Cortex Compared with HI/veh	Hippocampus Compared with sham	Hippocampus Compared with HI/veh
p-ULK-1 S555	5	HI/veh	↓	…	…	…
		HI/mel	…	↑	↑	↑
	24	HI/veh	↑	…	↑	…
		HI/mel	↑	↓	↑	↑
p-ULK-1 S757	5	HI/veh	↓	…	↓	…
		HI/mel	↓	↓	↓	↑
	24	HI/veh	↑	…	↓	…
		HI/mel	↓	↓	↓	…
LC3	5	HI/veh	…	…	…	…
		HI/mel	↓	↓	…	…
	24	HI/veh	↑	…	…	…
		HI/mel	↓	↓	↓	↓
p62	5	HI/veh	…	…	…	…
		HI/mel	…	…	↓	↓
	24	HI/veh	…	…	↓	…
		HI/mel	↓	↓	↓	↓

↑↓ = Significant change.

HI/mel indicates hypoxia–ischemia melatonin solution-treated group; HI/veh, hypoxia–ischemia vehicle solution-treated group; LC3, microtubule-associated protein 1 light chain 3; p62, sequestosome 1; p-ULK-1 (S555), phosphorylated ULK-1 serine 555; p-ULK-1 (S757): phosphorylated ULK-1 serine 757; and ULK-1, uncoordinated-51-like kinase 1.

mechanisms, such as antioxidant defense, improvement of energy metabolism, and immune function, as well as anti-inflammatory, antiapoptotic, and antiexcitotoxic effects.[62,63] It is important to note the complexity at the receptor levels involved in the melatonin mechanism, and a fascinating characteristic of these receptors is their capacity to form homo- and heteromers between each other and other G protein-coupled receptors, representing novel pharmacological entities to also consider.[64–66] At the moment, evidence showing that the activation of melatonin receptors is involved in neuroprotection is unclear. In early onset fetal growth restriction, where melatonin was administered to the mother, the fetal brain structure improved, showing no significant changes in melatonin receptor (MT)1 and MT2 receptors.[67] In a mouse model of stroke, a novel endogenous receptor, RAR-related orphan receptor alpha, has been suggested to be a pivotal mediator of the neuroprotective effect of melatonin.[68] Recently, the use of a specific agonist for MT1 receptors was shown to be neuroprotective in a mouse model of middle cerebral artery occlusion.[69,70]

It has been demonstrated that hMT1 (human MT1) and hMT2 (human MT2) receptors show similar pharmacological properties during their resting phases, and their differences appear during G-protein coupling,[71] which is an event that occurs spontaneously and as a preactivated structure on the membrane in heterologous systems.[71] On the other side, MT2 receptors could be expressed more easily than MT1 receptors in heterologous systems, so the number of binding zones could also correlate with that.[71] It has previously been shown that if melatonin levels rise above receptor saturation, which has been shown to be approximately 10 and 9.5 pKi values for hMT1 and hMT2,[72,73] the receptor-mediated effect of melatonin may not extend

Figure 10.   **LC3 and p62 regulations on treatment.**
A, Representative Western blot images of total LC3 bands and β-actin bands in the cortex at 5 and 24 hours after HI. **B**, Plot of the ratio of LC3 to β-actin in the cortex at 5 and 24 hours after HI. β-actin was used for loading control. **C**, Representative Western blot images of total p62 bands and β-actin bands in the cortex at 5 and 24 hours after HI. **D**, Plot of the ratio of p62 to β-actin in the cortex at 5 and 24 hours after HI. β-actin was used for loading control. **E**, Representative Western blot images of total LC3 bands and β-actin bands in the hippocampus at 5 and 24 hours after HI. **F**, Plot of the ratio of LC3 to β-actin in the hippocampus at 5 and 24 hours after HI. β-actin was used for loading control. **G**, Representative Western blot images of total p62 bands and β-actin bands in the hippocampus at 5 and 24 hours after HI. **H**, Plot of the ratio of p62 to β-actin in the hippocampus at 5 and 24 hours after HI. β-actin was used for loading control. Ordinary 1-way ANOVA tests (using the Tukey multiple comparison test) were performed to analyze the data. *$P<0.05$. Sham n=9 vs HI/vehicle n=9 (5 hours) and n=9 (24 hours) vs HI/melatonin n=12 (5 hours) and n=12 (24 hours). Data are presented as the median (IQR). Sham (white rectangles), HI/vehicle (black dots), and HI/melatonin (blue dots). HI indicates hypoxia–ischemia; IQR, Interquartile range; LC3, microtubule-associated proteins 1A/1B light chain 3B; and P62, Protein 62.

beyond the saturation pKi values of the receptor, and therefore the effects of melatonin appear to be non-MT-receptor mediated.[74] Taking into account the fact that the serum and brain concentrations of melatonin in the pharmacokinetic data of our study are much higher than the physiological serum and brain concentrations of melatonin, we strongly believe that there is a neuro-protective effect independent of the receptor level in our current study. However, due to the complexity at the receptor level and considering the high concentration
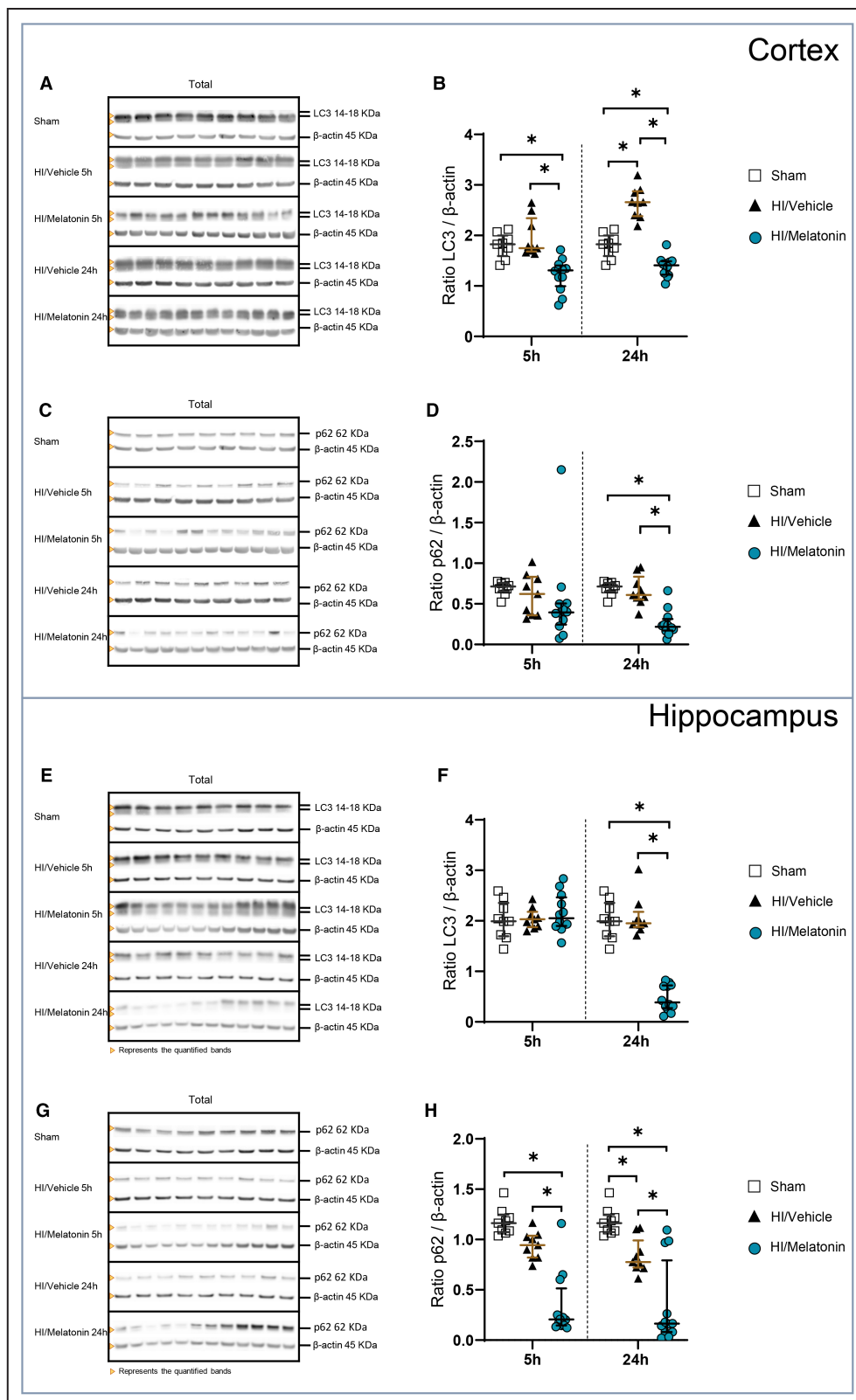
normally used of melatonin in animal models, we can assume that the observed effect could be nonreceptor related. Nevertheless, future experiments will be performed to characterize MT1 and MT2 receptor effects, using specific techniques for receptor characterization and specific antagonists for both receptors.

We demonstrated that melatonin treatment regulated autophagy via the AMPK/mTOR pathway. Our results showed that activation of mTOR can downregulate autophagy-related markers such as ULK-1, particularly at S757 phosphorylation, LC3, and p62, immediately after HI insult. We also demonstrated that downregulation of AMPK downregulates autophagy-related markers, such as ULK-1, particularly at S555 phosphorylation. It has been previously shown that mTOR interrupts the interaction of ULK-1 and AMPK, and causes the inhibition of autophagy in vitro.[52] However, there is insufficient evidence to show a direct effect of melatonin on autophagy, particularly in our model. Zhang and collaborators demonstrated that melatonin treatment inhibits autophagy via upregulation of NLRX1 (nucleotide-binding oligomerization domain and leucine-rich repeat-containing protein X1), which downregulates the mTOR activation, regulating mitophagy in a neonatal HI rat model.[59]

Our results provide new insights into the effects of melatonin on neonatal HIE, with a deeper understanding of the mechanism behind the effects observed after melatonin treatment and its use as a possible neuroprotective compound. These findings demonstrate that melatonin is a promising therapeutic agent against HIE, particularly in LMICs, where the use of TH does not show beneficial outcomes, or the treatment is not easily accessible. This study showed that the beneficial effects of melatonin are mediated through AMPK/mTOR/autophagy regulation and improvement of oligodendrogenesis. Although in our study we suggest melatonin as a potential neuroprotective agent, additional preclinical and clinical investigations are needed to further elucidate its neuroprotective effect.

CONCLUSIONS

Elucidation of the effect of melatonin on the AMPK/mTOR/autophagy pathway may increase our knowledge of the neuroprotective effects of melatonin in neonatal HIE. In this study, we validated that melatonin reduces global brain area loss, significantly increases myelination and oligodendrogenesis, and improves motor function. We also demonstrated that the neuroprotective effect of melatonin occurs through the AMPK/mTOR pathway after a neonatal HI insult. Considering the beneficial effects of melatonin and the results of our study, melatonin may be a potential drug for the treatment of neonatal HIE cases, particularly in LMICs.

REFERENCES

1. Perin J, Mulick A, Yeung D, Villavicencio F, Lopez G, Strong KL, Prieto-Merino D, Cousens S, Black RE, Liu L. Global, regional, and national causes of under-5 mortality in 2000–19: an updated systematic analysis with implications for the sustainable development goals. *Lancet Child Adolesc Health*. 2022;6:106–115. doi: 10.1016/S2352-4642(21)00311-4

2. Greco P, Nencini G, Piva I, Scioscia M, Volta CA, Spadaro S, Neri M, Bonaccorsi G, Greco F, Cocco I, et al. Pathophysiology of hypoxic–ischemic encephalopathy: a review of the past and a view on the future. *Acta Neurol Belg*. 2020;120:277–288. doi: 10.1007/s13760-020-01308-3

3. Millar LJ, Shi L, Hoerder-Suabedissen A, Molnár Z. Neonatal hypoxia ischaemia: mechanisms, models, and therapeutic challenges. *Front Cell Neurosci*. 2017;11. doi: 10.3389/fncel.2017.00078

4. Wassink G, Davidson JO, Dhillon SK, Zhou K, Bennet L, Thoresen M, Gunn AJ. Therapeutic hypothermia in neonatal hypoxic-ischemic encephalopathy. *Curr Neurol Neurosci Rep*. 2019;19. doi: 10.1007/s11910-019-0916-0

5. Sabir H, Scull-Brown E, Liu X, Thoresen M. Immediate hypothermia is not neuroprotective after severe hypoxia-ischemia and is deleterious when delayed by 12 hours in neonatal rats. *Stroke*. 2012;43:3364–3370. doi: 10.1161/STROKEAHA.112.674481

6. Thayyil S, Pant S, Montaldo P, Shukla D, Oliveira V, Ivain P, Bassett P, Swamy R, Mendoza J, Moreno-Morales M, et al. Hypothermia for moderate or severe neonatal encephalopathy in low-income and middle-income countries (helix): a randomised controlled trial in India, Sri Lanka, and Bangladesh. *Lancet Glob Health*. 2021;9:e1273–e1285. doi: 10.1016/S2214-109X(21)00264-3

7. Guidelines for perinatal care (eighth edition)/American Academy of Pediatrics [and] the American College of Obstetricians and Gynecologists. 2017.

8. Nair J, Kumar V. Current and emerging therapies in the management of hypoxic ischemic encephalopathy in neonates. *Children*. 2018;5. doi: 10.3390/children5070099

9. Inoki K, Kim J, Guan KL. Ampk and mtor in cellular energy homeostasis and drug targets. *Annu Rev Pharmacol Toxicol*. 2012;52:381–400. doi: 10.1146/annurev-pharmtox-010611-134537

10. Showkat M, Beigh MA, Andrabi KI. Mtor signaling in protein translation regulation: implications in cancer genesis and therapeutic interventions. *Mol Biol Int*. 2014;2014:1–14. doi: 10.1155/2014/686984

11. Lutz BM, Nia S, Xiong M, Tao Y-X, Bekker A. Mtor, a new potential target for chronic pain and opioid-induced tolerance and hyperalgesia. *Mol Pain*. 2015;11:s12990-015-0030.0. doi: 10.1186/s12990-015-0030-5

12. Ronnett GV, Ramamurthy S, Kleman AM, Landree LE, Aja S. Ampk in the brain: its roles in energy balance and neuroprotection. *J Neurochem*. 2009;109:17–23. doi: 10.1111/j.1471-4159.2009.05916.x

13. Qin X, Jiang B, Zhang Y. 4e-bp1, a multifactor regulated multifunctional protein. *Cell Cycle*. 2016;15:781–786. doi: 10.1080/15384101.2016.1151581

14. Magnuson B, Ekim B, Fingar DC. Regulation and function of ribosomal protein s6 kinase (s6k) within mtor signalling networks. *Biochem J*. 2011;441:1–21. doi: 10.1042/BJ20110892

15. Albanese F, Novello S, Morari M. Autophagy and lrrk2 in the aging brain. *Front Neurosci*. 2019;13:1352. doi: 10.3389/fnins.2019.01352

16. Russell RC, Yuan HX, Guan KL. Autophagy regulation by nutrient signaling. *Cell Res*. 2014;24:42–57. doi: 10.1038/cr.2013.166

17. Zhang Z, Yao L, Yang J, Wang Z, Du G. Pl3K/AKT and HIF-1 signaling pathway in hypoxia-ischemia (review). *Mol Med Rep*. 2018. doi: 10.3892/mmr.2018.9375

18. Weichhart T, Costantino G, Poglitsch M, Rosner M, Zeyda M, Stuhlmeier KM, Kolbe T, Stulnig TM, Hörl WH, Hengstschläger M, et al. The tsc-mtor signaling pathway regulates the innate inflammatory response. *Immunity*. 2008;29:565–577. doi: 10.1016/j.immuni.2008.08.012

19. Balduini W, Carloni S, Perrone S, Bertrando S, Tataranno ML, Negro S, Proietti F, Longini M, Buonocore G. The use of melatonin in hypoxic-ischemic brain damage: an experimental study. *J Matern Fetal Neonatal Med*. 2012;25(Suppl 1):119–124. doi: 10.3109/14767058.2012.663232

20. Hardeland R. Aging, melatonin, and the pro- and anti-inflammatory networks. *Int J Mol Sci*. 2019;20. doi: 10.3390/ijms20051223

21. Pevet P. Melatonin. *Dialogues Clin Neurosci*. 2002;4:57–72. doi: 10.31887/DCNS.2002.4.1/ppevet

22. Pang R, Advic-Belltheus A, Meehan C, Fullen DJ, Golay X, Robertson NJ. Melatonin for neonatal encephalopathy: from bench to bedside. *Int J Mol Sci*. 2021;22:22. doi: 10.3390/ijms22115481

23. Biran V, Phan Duy A, Decobert F, Bednarek N, Alberti C, Baud O. Is melatonin ready to be used in preterm infants as a neuroprotectant? *Dev Med Child Neurol*. 2014;56:717–723. doi: 10.1111/dmcn.12415

24. Ramos E, Patiño P, Reiter RJ, Gil-Martín E, Marco-Contelles J, Parada E, de los Rios C, Romero A, Egea J. Ischemic brain injury: new insights on the protective role of melatonin. *Free Radic Biol Med* 2017;104:32–53, DOI: 10.1016/j.freeradbiomed.2017.01.005

25. Ehlting A, Zweyer M, Maes E, Schleehuber Y, Doshi H, Sabir H, Bernis ME. Impact of hypoxia-ischemia on neurogenesis and structural and functional outcomes in a mild–moderate neonatal hypoxia-ischemia brain injury model. *Lifestyles*. 2022;12. doi: 10.3390/life12081164

26. Bernis ME, Zweyer M, Maes E, Schleehuber Y, Sabir H. Neutrophil extracellular traps release following hypoxic-ischemic brain injury in newborn rats treated with therapeutic hypothermia. *Int J Mol Sci*. 2023;24. doi: 10.3390/ijms24043598

27. Wood T, Osredkar D, Puchades M, Maes E, Falck M, Flatebo T, Walloe L, Sabir H, Thoresen M. Treatment temperature and insult severity influence the neuroprotective effects of therapeutic hypothermia. *Sci Rep*. 2016;6:23430. doi: 10.1038/srep23430

28. Pang R, Avdic-Belltheus A, Meehan C, Martinello K, Mutshiya T, Yang Q, Sokolska M, Torrealdea F, Hristova M, Bainbridge A, et al. Melatonin and/or erythropoietin combined with hypothermia in a piglet model of perinatal asphyxia. *Brain Commun*. 2021;3. doi: 10.1093/braincomms/fcaa211

29. Sabir H, Maes E, Zweyer M, Schleehuber Y, Imam FB, Silverman J, White Y, Pang R, Pasca AM, Robertson NJ, et al. Comparing the efficacy in reducing brain injury of different neuroprotective agents following neonatal hypoxia–ischemia in newborn rats: a multi-drug randomized controlled screening trial. *Sci Rep*. 2023;13. doi: 10.1038/s41598-023-36653-9

30. Vannucci SJ, Back SA. The vannucci model of hypoxic-ischemic injury in the neonatal rodent: 40 years later. *Dev Neurosci*. 2022;1–8:186–193. doi: 10.1159/000523990

31. Patel SD, Pierce L, Ciardiello A, Hutton A, Paskewitz S, Aronowitz E, Voss HU, Moore H, Vannucci SJ. Therapeutic hypothermia and hypoxia-ischemia in the term-equivalent neonatal rat: characterization of a translational preclinical model. *Pediatr Res*. 2015;78:264–271. doi: 10.1038/pr.2015.100

32. Griffin JM, Hingorani Jai Prakash S, Bockemuhl T, Benner JM, Schaffran B, Moreno-Manzano V, Buschges A, Bradke F. Rehabilitation enhances epothilone-induced locomotor recovery after spinal cord injury. *Brain Commun*. 2023;5:fcad005. doi: 10.1093/braincomms/fcad005

33. Li L, Qu Y, Li J, Xiong Y, Mao M, Mu D. Relationship between hif-1α expression and neuronal apoptosis in neonatal rats with hypoxia–ischemia brain injury. *Brain Res*. 2007;1180:133–139. doi: 10.1016/j.brainres.2007.08.059

34. Fan X, Heijnen CJ, van der Kooij MA, Groenendaal F, van Bel F. The role and regulation of hypoxia-inducible factor-1α expression in brain development and neonatal hypoxic–ischemic brain injury. *Brain Res Rev*. 2009;62:99–108. doi: 10.1016/j.brainresrev.2009.09.006

35. Conway JM, Walsh BH, Boylan GB, Murray DM. Mild hypoxic ischaemic encephalopathy and long term neurodevelopmental outcome—a systematic review. *Early Hum Dev*. 2018;120:80–87. doi: 10.1016/j.earlhumdev.2018.02.007

36. Goswami IR, Whyte H, Wintermark P, Mohammad K, Shivananda S, Louis D, Yoon EW, Shah PS. Canadian neonatal network I. Characteristics and short-term outcomes of neonates with mild hypoxic-ischemic encephalopathy treated with hypothermia. *J Perinatol*. 2020;40:275–283. doi: 10.1038/s41372-019-0551-2

37. Nakwa FL, Sepeng L, van Kwawegen A, Thomas R, Seake K, Mogajane T, Ntuli N, Ondongo-Ezhet C, Kesting S, Kgwadi DM, et al. Characteristics and outcomes of neonates with intrapartum asphyxia managed with therapeutic hypothermia in a public tertiary hospital in South Africa. *BMC Pediatr*. 2023;23:51. doi: 10.1186/s12887-023-03852-2

38. Bona E, Hagberg H, Løberg EM, Bågenholm R, Thoresen M. Protective effects of moderate hypothermia after neonatal hypoxia-ischemia: short- and long-term outcome. *Pediatr Res*. 1998;43:738–745. doi: 10.1203/00006450-199806000-00005

39. Diggikar S, Krishnegowda R. Therapeutic hypothermia for neonatal encephalopathy in low- and middle-income countries: a literature review. *J Trop Pediatr*. 2022;68:68. doi: 10.1093/tropej/fmac016

40. Garcia-Alix A, Arnaez J, Herranz-Rubia N, Alarcón A, Arca G, Valverde E, Blanco D, Lubian S. Ten years since the introduction of therapeutic hypothermia in neonates with perinatal hypoxic-ischaemic encephalopathy in Spain. *Neurologia (English Edition)*. 2022;38:364–371. doi: 10.1016/j.nrleng.2020.05.024

41. Hardeland R, Pandi-Perumal SR, Cardinali DP. Melatonin. *Int J Biochem Cell Biol*. 2006;38:313–316. doi: 10.1016/j.biocel.2005.08.020

42. Kilic E, Kilic U, Yulug B, Hermann DM, Reiter RJ. Melatonin reduces disseminate neuronal death after mild focal ischemia in mice via inhibition of caspase-3 and is suitable as an add-on treatment to tissue-plasminogen activator. *J Pineal Res*. 2004;36:171–176. doi: 10.1046/j.1600-079X.2003.00115.x

43. Drury PP, Davidson JO, Bennet L, Booth LC, Tan S, Fraser M, van den Heuij LG, Gunn AJ. Partial neural protection with prophylactic low-dose melatonin after asphyxia in preterm fetal sheep. *J Cereb Blood Flow Metab*. 2013;34:126–135. doi: 10.1038/jcbfm.2013.174

44. Robertson NJ, Lingam I, Meehan C, Martinello KA, Avdic-Belltheus A, Stein L, Tachrount M, Price D, Sokolska M, Bainbridge A, et al. High-dose melatonin and ethanol excipient combined with therapeutic hypothermia in a newborn piglet asphyxia model. *Sci Rep*. 2020;10:10. doi: 10.1038/s41598-020-60858-x

45. Robertson NJ, Faulkner S, Fleiss B, Bainbridge A, Andorka C, Price D, Powell E, Lecky-Thompson L, Thei L, Chandrasekaran M, et al. Melatonin augments hypothermic neuroprotection in a perinatal asphyxia model. *Brain*. 2013;136:90–105. doi: 10.1093/brain/aws285

46. Pang R, Han HJ, Meehan C, Golay X, Miller SL, Robertson NJ. Efficacy of melatonin in term neonatal models of perinatal hypoxia-ischaemia. *Ann Clin Transl Neurol*. 2022;9:795–809. doi: 10.1002/acn3.51559

47. Berger HR, Nyman AKG, Morken TS, Wideroe M. Transient effect of melatonin treatment after neonatal hypoxic-ischemic brain injury in rats. *PLoS One*. 2019;14:e0225788. doi: 10.1371/journal.pone.0225788

48. Yeleswaram K, McLaughlin LG, Knipe JO, Schabdach D. Pharmacokinetics and oral bioavailability of exogenous melatonin in preclinical animal models and clinical implications. *J Pineal Res*. 1997;22:45–51. doi: 10.1111/j.1600-079X.1997.tb00302.x

49. Reiling JH, Sabatini DM. Stress and mtorture signaling. *Oncogene*. 2006;25:6373–6383. doi: 10.1038/sj.onc.1209889

50. Rousset CI, Leiper FC, Kichev A, Gressens P, Carling D, Hagberg H, Thornton C. A dual role for amp-activated protein kinase (ampk) during neonatal hypoxic–ischaemic brain injury in mice. *J Neurochem*. 2015;133:242–252. doi: 10.1111/jnc.13034

51. Williams T, Courchet J, Viollet B, Brenman JE, Polleux F. Amp-activated protein kinase (ampk) activity is not required for neuronal development but regulates axogenesis during metabolic stress. *Proc Natl Acad Sci*. 2011;108:5849–5854. doi: 10.1073/pnas.1013660108

52. Kim J, Kundu M, Viollet B, Guan K-L. Ampk and mtor regulate autophagy through direct phosphorylation of ulk1. *Nat Cell Biol*. 2011;13:132–141. doi: 10.1038/ncb2152

53. Chen H, Xiong T, Qu Y, Zhao F, Ferriero D, Mu D. Mtor activates hypoxia-inducible factor-1α and inhibits neuronal apoptosis in the developing rat brain during the early phase after hypoxia–ischemia. *Neurosci Lett*. 2012;507:118–123. doi: 10.1016/j.neulet.2011.11.058

54. Carriere A, Romeo Y, Acosta-Jaquez HA, Moreau J, Bonneil E, Thibault P, Fingar DC, Roux PP. Erk1/2 phosphorylate raptor to promote ras-dependent activation of mtor complex 1 (mtorc1). *J Biol Chem*. 2011;286:567–577. doi: 10.1074/jbc.M110.159046

55. Keane L, Antignano I, Riechers S-P, Zollinger R, Dumas AA, Offermann N, Bernis ME, Russ J, Graelmann F, McCormick PN, et al. Mtor-dependent translation amplifies microglia priming in aging mice. *J Clin Invest*. 2021;131. doi: 10.1172/JCI155208

56. Dumbuya JS, Chen L, Shu SY, Ma L, Luo W, Li F, Wu J-Y, Wang B. G-csf attenuates neuroinflammation and neuronal apoptosis via the mtor/p70sk6 signaling pathway in neonatal hypoxia-ischemia rat model. *Brain Res*. 2020;1739:146817. doi: 10.1016/j.brainres.2020.146817

57. Xue H, Xu Y, Wang S, Wu ZY, Li XY, Zhang YH, Niu JY, Gao QS, Zhao P. Sevoflurane post-conditioning alleviates neonatal rat hypoxic-ischemic cerebral injury via ezh2-regulated autophagy. *Drug Des Devel Ther*. 2019;13:1691–1706. doi: 10.2147/DDDT.S197325

58. Xu YH, Xu JB, Chen LL, Su W, Zhu Q, Tong GL. Protective mechanisms of quercetin in neonatal rat brain injury induced by hypoxic-ischemic brain damage (hibd). *Food Sci Nutr*. 2023;11:7649–7663. doi: 10.1002/fsn3.3684

59. Zhang Y, Chen D, Wang Y, Wang X, Zhang Z, Xin Y. Neuroprotective effects of melatonin-mediated mitophagy through nucleotide-binding oligomerization domain and leucine-rich repeat-containing protein x1 in neonatal hypoxic-ischemic brain damage. *FASEB J*. 2023;37:e22784. doi: 10.1096/fj.202201523R

60. Koh PO. Melatonin prevents ischemic brain injury through activation of the mtor/p70s6 kinase signaling pathway. *Neurosci Lett*. 2008;444:74–78. doi: 10.1016/j.neulet.2008.08.024

61. Ding K, Wang H, Xu J, Lu X, Zhang L, Zhu L. Melatonin reduced microglial activation and alleviated neuroinflammation induced neuron degeneration in experimental traumatic brain injury: possible involvement of mtor pathway. *Neurochem Int*. 2014;76:23–31. doi: 10.1016/j.neuint.2014.06.015

62. Cardinali DP. An assessment of melatonin's therapeutic value in the hypoxic-ischemic encephalopathy of the newborn. *Front Synaptic Neurosci*. 2019;11:11. doi: 10.3389/fnsyn.2019.00034

63. Cardinali DP. Melatonin: clinical perspectives in neurodegeneration. *Front Endocrinol (Lausanne)*. 2019;10:480. doi: 10.3389/fendo.2019.00480

64. Cecon E, Oishi A, Jockers R. Melatonin receptors: molecular pharmacology and signalling in the context of system bias. *Br J Pharmacol*. 2018;175:3263–3280. doi: 10.1111/bph.13950

65. Reiter RJ, Tan DX, Manchester LC, Terron MP, Flores LJ, Koppisepi S. Medical implications of melatonin: receptor-mediated and receptor-independent actions. *Adv Med Sci*. 2007;52.

66. Tse LH, Wong YH. Modeling the heterodimer interfaces of melatonin receptors. *Front Cell Neurosci*. 2021;15:725296. doi: 10.3389/fncel.2021.725296

67. Malhotra A, Rocha A, Yawno T, Sutherland AE, Allison BJ, Nitsos I, Pham Y, Jenkin G, Castillo-Melendez M, Miller SL. Neuroprotective effects of maternal melatonin administration in early-onset placental insufficiency and fetal growth restriction. *Pediatr Res*. 2024;95:1510–1518. doi: 10.1038/s41390-024-03027-4

68. Zang M, Zhao Y, Gao L, Zhong F, Qin Z, Tong R, Ai L, Petersen L, Yan Y, Gao Y, et al. The circadian nuclear receptor roralpha negatively regulates cerebral ischemia-reperfusion injury and mediates the neuroprotective effects of melatonin. *Biochim Biophys Acta Mol basis Dis*. 2020;1866:165890. doi: 10.1016/j.bbadis.2020.165890

69. Zhang X, Peng B, Zhang S, Wang J, Yuan X, Peled S, Chen W, Ding J, Li W, Zhang A, et al. The mt1 receptor as the target of ramelteon neuroprotection in ischemic stroke. *J Pineal Res*. 2024;76:e12925. doi: 10.1111/jpi.12925

70. Wu XL, Lu SS, Liu MR, Tang WD, Chen JZ, Zheng YR, Ahsan A, Cao M, Jiang L, Hu WW, et al. Melatonin receptor agonist ramelteon attenuates mouse acute and chronic ischemic brain injury. *Acta Pharmacol Sin*. 2020;41:1016–1024. doi: 10.1038/s41401-020-0361-2

71. Legros C, Devavry S, Caignard S, Tessier C, Delagrange P, Ouvry C, Boutin JA, Nosjean O. Melatonin mt(1) and mt(2) receptors display different molecular pharmacologies only in the g-protein coupled state. *Br J Pharmacol*. 2014;171:186–201. doi: 10.1111/bph.12457

72. Kato K, Hirai K, Nishiyama K, Uchikawa O, Fukatsu K, Ohkawa S, Kawamata Y, Hinuma S, Miyamoto M. Neurochemical properties of ramelteon (tak-375), a selective mt1/mt2 receptor agonist. *Neuropharmacology*. 2005;48:301–310. doi: 10.1016/j.neuropharm.2004.09.007

73. Hardeland R. Investigational melatonin receptor agonists. *Expert Opin Investig Drugs*. 2010;19:747–764. doi: 10.1517/13543784.2010.482926

74. Hardeland R. Divergent importance of chronobiological considerations in high- and low-dose melatonin therapies. *Diseases*. 2021;9. doi: 10.3390/diseases9010018